Lectures on the Physics of Highly Correlated Electron Systems, AIP Conference Proceedings 438.
Ed. F. Mancini (1998)

Quantum Dissipative Systems

F. Guinea*, E. Bascones*† and M.J. Calderon*

*Instituto de Ciencia de Materiales de Madrid (CSIC). 28049 Cantoblanco, Madrid, Spain.
†Departamento de Física de la Materia Condensada. Universidad Autónoma de Madrid. 28049 Cantoblanco, Madrid, Spain.

INTRODUCTION

One of the most interesting topic of quantum mechanics is the study of open quantum systems. By it, we mean a simple quantum system, described by one or a few degrees of freedom, interacting with a background characterized by a continuum of excitations. If the number of low density excitations of the extended system is large enough, and their coupling to the simple system is the right one, the properties of both are changed in a substantial way. New features emerge, which are difficult to glimpse from the consideration of each system separately. The standard decomposition of such a problem into two decoupled subsystems plus a weak perturbation breaks down.

Moreover, this kind of problem is ubiquitous in many areas of physics. The required features in the extended system are those found in normal metals: a continuum of low energy excitations, the electron-hole pairs, whose number increases linearly with energy[1].

The coupling required is also not too restrictive. Low energy excitations should be more weakly coupled than high energy ones. The dependence of the coupling on energy is typical of impurity problems. Low energy excitations are more delocalized and, hence, less coupled to a finite system. As it will be seen below, the systems which share the features described here encompass a much broader spectrum. The system with few degrees of freedom needs not be a microscopic impurity. Many devices are characterized by a few, collective degrees of freedom[2]. It is well known that a macroscopic system, in contact with a reservoir, experiences random fluctuations and friction. We will see how similar phenomena arise in the quantum limit, when the degrees of freedom of the macroscopic device need to be treated within quantum mechanics.

A particular class of systems for which the methods discussed here are applicable are those mesoscopic devices which, at high temperatures, behave like ordinary

---

1) note that a system with a *constant* density of excitations at low energies is unstable against any perturbation, while a metal is a well defined state of matter, as first shown by L. D. Landau.
2) the simplest case being the classical pendulum, always described in terms of the coordinates of its center of mass.

ohmic resistors. If the dimensions of these devices are small enough, the macroscopic parameters which describe them, charges, currents, superconducting phases, can show distinct quantum behavior at low temperatures. The ohmic resistors give rise to a coupling to an additional set of degrees of freedom which cannot be ignored.

The following section presents the simplest situation where the physics loosely described here can be studied in detail, the so called orthogonality catastrophe, which arises in X-ray photoemission in metals. The insight gained there is used to analyze the canonical model in this class of systems: the dissipative two level system. We show, in the following section, how the insight gained from that model can be used to tackle one of the most known of all problems in condensed matter physics, the Kondo problem. Then, we will move to macroscopic systems, and we first discuss the standard treatments of friction in the quantum limit. In the last section, we apply the previous knowledge to a broad class of mesoscopic devices, characterized by strong charging effects (Coulomb blockade).

We will not follow chronological order, for pedagogical reasons. Throughout the notes, the method of choice is the renormalization group, in its many guises. It must be noted, however, that many of the models have also been solved by Bethe ansatz techniques, and that conformal field methods have been used to gain insight into their behavior. References to these works are given. We apologize, however, for not presenting in full these treatments. We esteem that, in any case, the renormalization group has proved to be a very powerful theoretical tool, whose usefulness extends well beyond the present problems. In addition, it provides a very general framework which allows us, in a clear fashion, to relate and classify the systems described below.

We gratefully acknowledge the Low Temperature Laboratory of the Universidad Autónoma de Madrid for providing us the experimental curves of charging effects on superconductors.

I ORTHOGONALITY CATASTROPHE

Introduction

One of the simplest examples of the effects of the interaction between a simple quantum system, described by one or few degrees of freedom, and an extended system, characterized by a continuum of excitations, is the response of the electrons in a metal when a local potential is suddenly switched on inside the metal. This situation describes, for instance, the creation of a hole in the core level of an atom inside the metal, in an X-ray absorption process.

The most striking feature of the analysis is that the ground states of the system with and without the local potential, i.e. with and without the core level, are orthogonal. Hence, the sudden switching of the potential cannot lead to a transition between the old and the new ground states [1,2]. The effect has been appropriately labeled *the orthogonality catastrophe*. If the potential is not localized, the orthogonality catastrophe is only observed in one dimensional systems. This leads to non-Fermi liquid behavior in quasi-1dimensional systems. Absorption of X-rays in metals must leave the metal in an excited state. Electron-hole pairs created by the process allow the forbidden transition to be observed.

The immediate consequence of the orthogonality catastrophe is the failure of perturbation theory. The new ground state cannot be obtained by making finite corrections to the old one.

Bosonization and orthogonality catastrophe

We can describe a metal as a Fermi liquid with a continuum spectrum. Under the Fermi energy all these levels are occupied (Fig. 1) so the excitations must involve transitions to the levels above the Fermi energy. The only degrees of freedom we are going to take into account in the description of a metal are these excitations.

The Hamiltonian for a free electron gas is:

$$H_o = \sum_k \epsilon_k c_k^\dagger c_k \tag{1}$$

where $c_k^\dagger$ y c_k are the creation and destruction operators, respectively. The ground state is $|\psi_o\rangle$.

When we add an impurity to the system, an extra term appears in the Hamiltonian. The impurity is represented as a *local potential*:

$$H_v = H_o + \sum_{k,k'} V_{kk'} c_k^\dagger c_{k'} \tag{2}$$

and the new ground state is $|\psi_v\rangle$.

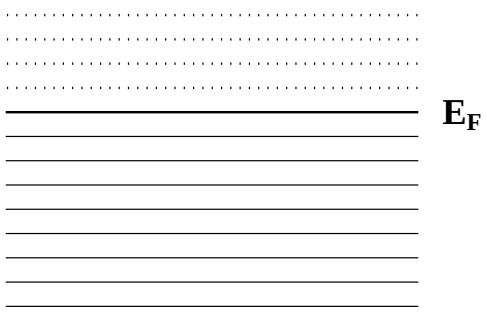

FIGURE 1. The metal is considered as a Fermi liquid such that all the levels are occupied under the Fermi energy. This implies that all the excitations must involve transitions to the levels above the Fermi energy.

Hamiltonians (1) and (2) must be viewed as effective Hamiltonians which describe the low energy excitations of the system. The range of values of k needs not include the full conduction band of the metal. In most cases, we are interested in processes at scales of 0.1eV and below, while typical bandwidths are of the order of 1eV. Hence, we consider only a narrow slice of states near the Fermi level. This implies that the Fourier components of the impurity potential involved in (2) is small. We make the approximation:

$$\sum_{k,k'} V_{kk'} c_k^\dagger c_{k'} \to \frac{V}{N} \sum_{k,k'} c_k^\dagger c_{k'} \tag{3}$$

We assume that the reservoir is macroscopic, so that we must take the thermodynamic limit, i.e. $N \to \infty$, where N is the number of levels in the system. $|\psi_o\rangle$ and $|\psi_v\rangle$ are constructed by monoelectronic wavefunctions so they are both Slater determinants. What we want to calculate is the overlap of two Slater determinants, which can be written as the determinant of the matrix built up by the overlaps of pairs of one electron wavefunctions:

$$\langle \psi_o | \psi_v \rangle = \begin{vmatrix} \langle \psi_1^o | \psi_1^v \rangle & \langle \psi_1^o | \psi_2^v \rangle & \ldots \\ \langle \psi_2^o | \psi_1^v \rangle & \langle \psi_2^o | \psi_2^v \rangle & \ldots \\ . & . & \\ . & . & \\ . & . & \end{vmatrix} \tag{4}$$

In our description, the spectrum of the free system consists on N levels equally spaced by a distance Δ (Fig. 2). Therefore, the bandwidth is $W = N\Delta$. When we take the thermodynamic limit ($N \to \infty$) we will take $\Delta \to 0$ in order to keep W finite.

With this picture in mind we can study the degeneracy of the low excitation spectrum of H_o (1). If we excite an electron from the Fermi level N to the first unnocupied level N+1, its energy of excitation is Δ. This is the only process with

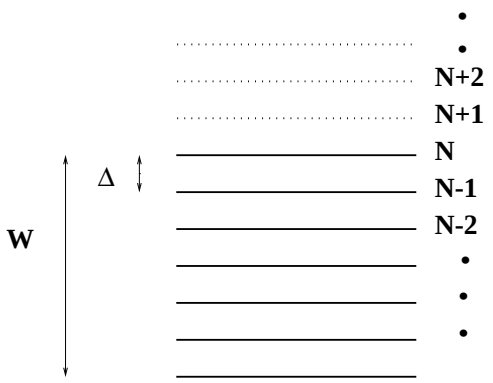

FIGURE 2. The spectrum of the free system consists on N levels equally spaced.

such energy, so its degeneracy is 1. Now we look for the processes with an excitation energy 2Δ. It is easy to see that there are two processes that lead to such energy. These are $N \to N+2$ and $N-1 \to N+1$. In this way, it is straightforward to study the whole excitation spectrum and the degeneracy of the levels. These set of energies and levels also arise in problems of harmonic oscillators [3]. So we can think on bosonizing our fermionic problem, by making the correspondence:

$$\sum_k \epsilon_k c_k^\dagger c_k \to \sum_{n=1}^{N} \Delta n b_n^\dagger b_n \tag{5}$$

where $b_n^\dagger$ creates an excited state with energy Δn. For our regime of low energies the number of electrons in the electronic Hamiltonian is of the same order as the number of levels in the bosonic one. Although these two quantities are not exactly equal, the difference is unimportant in the thermodynamic limit ($N \to \infty$).

The correspondence breaks down at high energies, where we excite electrons from the bottom of the band. We expect these effects to be negligible at sufficiently low scales. In the renormalization group philosophy, the model is only useful in order to obtain universal quantities, that is, those which are almost independent of the choice of high energy cutoff[4].

We have another term in the Hamiltonian H_v (2) to bosonize. This term can be rewritten as:

$$\sum_n \sum_m c_{n+m}^\dagger c_m \tag{6}$$

where we have only changed the notation in order to make more transparent the connection with the bosonic Hamiltonian. For each n, we are considering all ex-

---

[3] The first excited state with energy Δ is achieved by applying the operator $b_1^\dagger$ to the ground state. The second excited state with energy 2Δ corresponds to the application of both $b_2^\dagger$ or $b_1^{\dagger 2}$ to the ground state... Not only the values of the energy of the excitation levels are the same but also their degeneracies.

[4] note that, in any case, a more realistic electronic model should include variations in the density of states, and band edge effects, which are not included in (2)

citations with energy $n\Delta$. These operators obey commutation relations almost equivalent to those of bosons, $[b_n, b_m^\dagger] = \delta_{nm}$, when the bottom of the band is occupied.

The commutation relation is:

$$\begin{aligned}
&[\ \textstyle\sum_m\ c_{n+m}^\dagger c_m, \sum_{m'} c_{n'+m'}^\dagger c_{m'}] = \\
&= \textstyle\sum_{mm'} c_{n+m}^\dagger c_{m'} \delta_{m,m'+n'} - \sum_{mm'} c_{n'+m'}^\dagger c_m \delta_{m',m+n} = \\
&= \textstyle\sum_{mm'} (c_{n+m}^\dagger c_{m-n'} - c_{m+n+n'}^\dagger c_m) = \\
&= \textstyle\sum_{mm''} (c_{m''+n+n'}^\dagger c_{m''} - c_{m+n+n'}^\dagger c_m)
\end{aligned} \tag{7}$$

This is 0 provided $n + n' \neq 0$,namely, the bottom of the band is occupied.

If $n + n' = 0$, namely, $n = 0$ and $n' = 0$, we are at the bottom of the band. In this case:

$$\sum_{m,m''} (c_{m''}^\dagger c_{m''} - c_m^\dagger c_m) = 0 \tag{8}$$

except for $m = 0$ when we have (let us write $m'' = m + n$):

$$c_n^\dagger c_n - c_0^\dagger c_0 \tag{9}$$

If we project this into the ground state, the commutation relation gives n because both terms are simply numbers. Hence, by dividing the operators in the right hand side by n, this expression can be cast as that satisfied by bosons. We define:

$$b_n^\dagger = \frac{1}{\sqrt{n}} \sum_m c_{m+n}^\dagger c_m, \tag{10}$$

Now we can write a bosonic Hamiltonian with a linear interaction term:

$$H = \sum_{n=1}^{N} \Delta n b_n^\dagger b_n + \frac{V}{N} \sum_n \sqrt{n}(b_n^\dagger + b_n). \tag{11}$$

And if we define:

$$b_n^\dagger = \tilde{b}_n^\dagger - \frac{V}{N} \frac{1}{\Delta\sqrt{n}} \tag{12}$$

the total Hamiltonian has a simpler form:

$$H = \sum_{n=1}^{N} \Delta n \tilde{b}_n^\dagger \tilde{b}_n. \tag{13}$$

(plus a constant which is not relevant because it only implies a shift in the ground state energy). Notice that this is the same Hamiltonian as the bosonized H_o except

for the tilde. Having this in mind is easy to understand that the operator U that makes the transformation $U^\dagger b_n^\dagger U = \tilde{b}_n^\dagger$ is the same that gives the transformation between the Hamiltonian with (H_v) and without (H_o) impurities:

$$U^\dagger H_v U = H_o \tag{14}$$

as well as a relation between the ground states of both Hamiltonians.

$$|\psi_v\rangle = U^\dagger |\psi_o\rangle. \tag{15}$$

The operator U which corresponds to this transformation is:

$$U = exp(-\sum_n \frac{V}{N}\frac{1}{\Delta\sqrt{n}}(b_n^\dagger - b_n)) \tag{16}$$

The overlap we want to calculate is the expected value of U in the ground state of the free system:

$$\langle\psi_v|\psi_o\rangle = \langle\psi_o|U|\psi_o\rangle \tag{17}$$

To calculate this expression we use the normal ordering to make the destruction operators actuate first on the wave function.

Then the expression for U is:

$$U = exp(-\sum_n \frac{V}{N}\frac{1}{\Delta\sqrt{n}}b_n^\dagger)exp(\sum_n \frac{V}{N}\frac{1}{\Delta\sqrt{n}}b_n)exp(-\frac{1}{2}\sum_n(\frac{V}{N})^2\frac{1}{\Delta^2 n}) \tag{18}$$

Where we have used,

$$e^{A+B} = e^A e^B e^{-\frac{i}{2}[A,B]} \tag{19}$$

that is only valid if $[A, B]$ commutes with A and B.

When we apply this expression to $|\psi_o\rangle$ all the exponents with destruction operators vanish and when we apply it to $\langle\psi_o|$ the same is achieved for the construction operators. Consequently, the only term that survives is:

$$\langle\psi_o|U|\psi_o\rangle = exp(-\frac{1}{2}(\frac{V}{N\Delta})^2\sum_{n=1}^{N}\frac{1}{n}) = exp(-\frac{1}{2}(\frac{V}{N\Delta})^2 lnN) = N^{-\frac{1}{2}(\frac{V}{W})^2} \tag{20}$$

So in the thermodynamic limit the overlap goes to 0 and we find the orthogonality catastrophe as introduced before. In a real metal $N \sim 10^{23}$ and $\frac{V}{W} \sim 0.1 - 0.2$ so this limit is completely justified. The orthogonality catastrophe was first proved by Anderson [1] but he solved the electronic Hamiltonian rather than the bosonic giving the result in terms of a phase shift of the scattered wavefunction. The result is exactly the same if we put in (20) $\frac{\delta}{\pi}$ instead of $\frac{V}{W}$.

The previous result not only implies the failure of the perturbation expansion. It also gives a hint on the way the expansion fails. As the size of the system

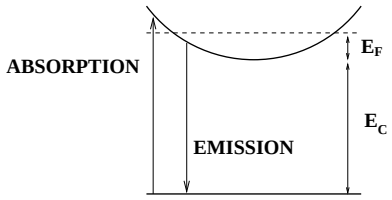

FIGURE 3. Schematic emission and absorption between core level and the conduction band in a metal.

grows, the lowest order corrections diverge as $ln(N)$, as you can see making the expansion of the exponential in eq. (20), where N is a measure of the total number of electrons. When the low energy part of the spectrum is decoupled from V, either by thermal fluctuations, by V dependence on time, etc., $ln(N)$ is replaced by $ln[\epsilon_c/max(\omega, T)]$. ϵ_c is the maximum energy available for the formation of electron-hole pairs, and ω and T are the driving frequency and the temperature at which the system is probed. This type of divergence has been extensively studied in quantum field theories where the number of degrees of freedom is infinite like in our problem. The logarithmic divergence leads to renormalizable models in which scale dependent couplings are defined, so they depend on the ratio ϵ_c and the scale of interest for the experimental situation (given, for example, by the temperature). This 'renormalizability' is a common feature of the models studied here and this fact will be used in subsequent chapters.

Edge singularities

The optical transitions in metals are related to photons of high energy: X-ray spectroscopy. If we use a one body picture, namely, we consider that the optical transitions do not change the energy bands, the emission and absorption spectra have a continuous form (Fig. 3). In the X-ray absorption processes, the energy of the photon is used to lift an electron from the occupied levels under the Fermi energy to an unoccupied level. The absorption starts at a threshold energy that is the minimum needed to excite an electron to the first unoccupied level. In the same way, the emission has a maximum energy in its spectrum.

In the absence of the orthogonality catastrophe, the observed spectrum should be a delta function[5] (see Fig. 4).

The orthogonality catastrophe implies that the weight of the delta peak vanishes. The whole spectrum is due to the emission of electron-hole pairs. These pairs require a finite energy to be created, and a broad structure is observed below the energy of the (absent) quasiparticle peak.

In the same way, the absorption spectrum presents lines above the energy of excitation because the transition must put the electron in an unoccupied level

---

[5)] plus an incoherent background at high energies, associated to the emission of phonons, plasmons ...

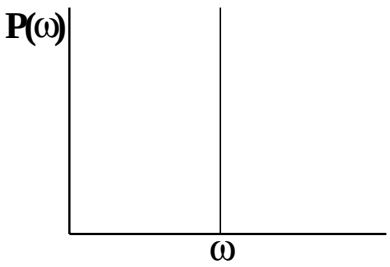

FIGURE 4. In a one-body picture, there is only one transition in the absorption spectrum and only one of the electrons is affected.

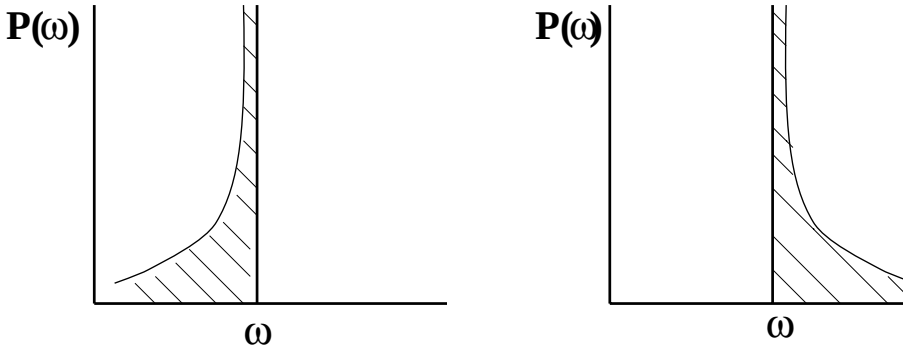

FIGURE 5. In a many body picture the spectra has a background of lines. On the left, emission and on the right, absorption.

that, due to the excited states produced by the orthogonality catastrophe, is at higher energy.

Mahan [2] showed that these spectra present a power law singularity at the energy threshold.

Photoemission spectrum

First, let us study the shape of the photoemission spectrum. We are going to use the notation introduced in the proof of the orthogonality catastrophe, namely, the Hamiltonians H_o (1) and H_v (2) and their ground states $|\psi_o\rangle$ and $|\psi_v\rangle$ such that the potential is the screened Coulomb interaction between the core hole and the electrons. We want to calculate:

$$P(\epsilon - \omega) = |\langle \psi_o | \psi_v \rangle|^2 \tag{21}$$

namely, the probability to create a process which leads to a final state with energy $\epsilon - \omega$. ϵ is the energy of the excited electrons and ω is the energy of $|\psi_v\rangle$. To facilitate the calculation let us introduce the Fourier transform of such probability:

$$P(t) = \int |\langle \psi_o | \psi_v \rangle|^2 e^{i\omega t} d\omega =$$

$$= \sum_{\omega} \langle \psi_o | \psi_v \rangle e^{i\omega t} \langle \psi_v | \psi_o \rangle$$
$$= \langle \psi_o | e^{iH_v t} | \psi_o \rangle \tag{22}$$

The last transformation can be done because $|\psi_v\rangle$ is the base that diagonalizes H_v.

We know from the previous section the operator U that relates H_o and H_v, so the last equation may be solved:

$$P(t) = \langle \psi_o | e^{iH_v t} | \psi_o \rangle = \langle \psi_o | U^\dagger e^{iH_o t} U | \psi_o \rangle$$
$$= \langle \psi_o | U^\dagger(t) U(o) | \psi_o \rangle \tag{23}$$

In the last step we have introduced $e^{iH_o t} e^{-iH_o t}$ on the right of the bra and on the left of the ket and we have used the fact that $|\psi_o\rangle$ is the basis that diagonalizes H_o. Now the expression for U is used:

$$P(t) = \langle \psi_o | U^\dagger(t) U(o) | \psi_o \rangle =$$
$$= \langle \psi_o | \exp(-\sum_n \frac{V}{N} \frac{1}{\Delta\sqrt{n}} b_n^\dagger e^{in\Delta t}) \exp(\sum_n \frac{V}{N} \frac{1}{\Delta\sqrt{n}} b_n e^{-in\Delta t})$$
$$\times \exp(-\sum_n \frac{V}{N} \frac{1}{\Delta\sqrt{n}} b_n^\dagger) \exp(\sum_n \frac{V}{N} \frac{1}{\Delta\sqrt{n}} b_n) | \psi_o \rangle \tag{24}$$

The first and the last exponents vanish when applied to the ground state (remember $b_n|\psi_o\rangle = 0$). The second and the third term are cast in normal order (construction operators to the left of the destruction ones) taking into account that $e^A e^B = e^B e^A e^{-\frac{i}{2}[A,B]}$. The first two exponentials give once again 1 and the only one that is left is $e^{-\frac{i}{2}[A,B]}$:

$$P(t) = \exp[\sum_n \frac{V}{N} \frac{1}{\Delta\sqrt{n}} b_n e^{-in\Delta t}] \exp[-\sum_n \frac{V}{N} \frac{1}{\Delta\sqrt{n}} b_n^\dagger] =$$
$$= \exp(\sum_n (\frac{V^2}{N^2})(\frac{e^{-in\Delta t} - 1}{\Delta^2 n})) = e^{(\frac{V}{N})^2 \log \Delta t} \sim (\Delta t)^{(\frac{V}{N})^2} \tag{25}$$

The exponential in the last expression, as it depends on n, kills the logarithmic divergence on N that we found on eq. (20). To calculate $P(\omega)$ we Fourier transform the previous equation:

$$P(\epsilon - \omega) \sim (\epsilon - \omega)^{-1 + (\frac{V}{N})^2} i = (\epsilon - \omega)^\alpha \tag{26}$$

Taking the thermodynamic limit, $(N \to \infty)$ $\alpha = -1$ and this probability diverges for $\epsilon = \omega$.

In the same way as in the orthogonality catastrophe, the exponent can be written as a function of the phase shifts of conduction electrons at the Fermi surface when they are scattered by the core hole [3].

X-ray absorption

We now analyze the problem of the *X-ray absorption*. As mentioned before, if the interactions with the medium are not taken into account, we would only observe the creation of an electron with the energy of the absorbed photon.

The probability function we have to calculate is:

$$P(\omega) = |\langle \psi_o | c_0^\dagger | \psi_v \rangle|^2 \tag{27}$$

where $c_0^\dagger$ creates an electron in the core level, namely, it takes a state of $n+1$ electrons into states of n electrons. As before, we make the Fourier transform of the probability:

$$\begin{aligned} P(t) &= \sum_w \langle \psi_0 | c_0^\dagger | \omega \rangle e^{i\omega t} \langle \omega | c_0 | \psi_0 \rangle = \\ &= \langle \psi_0 | c_0^\dagger e^{iH_v t} c_0 | \psi_0 \rangle = \\ &= \langle \psi_0 | c_0^\dagger(t) c_0(0) | \psi_0 \rangle \end{aligned} \tag{28}$$

The last expression is the propagator of the electron out of equilibrium. The wavefunctions of the core level have the form $|0, i\rangle$ where i is the index that gives us the number of electrons. To calculate $P(t)$ we need the commutation rules $[c_0, H_0]$ and $[c_0, V]$ because $H_v = H_0 + V$. To exploit the machinery developed in the previous section we have to express c_0 in terms of bosons:

$$c_0^\dagger = A \sigma^\dagger e^{\lambda \sum_n \frac{1}{\sqrt{n}} b_n^\dagger} \tag{29}$$

where $\sigma^\dagger$ acts on the index i and b_n is a boson operator.

We want this operator to have the same dynamics as the corresponding electron operator. This is achieved if its time correlator has the right behavior, that is:

$$\langle \psi_0 | c_0^\dagger(t) c_0(0) | \psi_0 \rangle \sim \frac{1}{t} \tag{30}$$

Using equation (29), (30) leads to:

$$\begin{aligned} &\langle \ \psi_0 | c_0^\dagger(t) c_0(0) | \psi_0 \rangle = \\ &= A^2 \langle \psi_0 | \exp(\lambda \sum_n \frac{e^{i\Delta n t}}{\sqrt{n}} b_n) \exp(\lambda \sum_n \frac{b_n^\dagger}{\sqrt{n}}) | \psi_0 \rangle = \\ &= A^2 \exp(\lambda^2 \sum_n \frac{e^{i\Delta n t}}{n}) = A^2 (\Delta t)^{\lambda^2} \end{aligned} \tag{31}$$

Here we have used the normal ordering. In order to achieve the behavior (30) λ^2 must be -1. If we consider the whole Hamiltonian H_v:

$$\langle\ \psi_0|c_0^\dagger e^{iH_v t}c_0|\psi_0\rangle =$$
$$= \langle\psi_0|U^\dagger A\exp(\lambda\sum_n \frac{e^{i\Delta nt}}{\sqrt{n}}b_n^\dagger)A\exp(\lambda\sum_n \frac{b_n}{\sqrt{n}})U|\psi_0\rangle \tag{32}$$

where we have used the operator U that relates the Hamiltonians H_0 and H_v. Applying normal ordering as usual is straightforward to achieve:

$$P(t) = (\Delta t)^{-(1+\frac{V}{W})^2} \tag{33}$$

So

$$P(\omega) \sim \omega^{-1+(1+\frac{V}{W})^2} = \omega^{\frac{2V}{W}+\frac{V^2}{W^2}} \tag{34}$$

The first term in the exponential is due to excitonic effects, namely, to interactions between the electron and the valence band hole, and the second to the orthogonality catastrophe. The former, usually makes the edges diverge while the latter gives convergence because the logarithmic divergence has disappeared. This result was computed first by Nozières and de Dominicis, directly in terms of the original electrons [3].

The solution we have discussed is asymptotically exact near the edge. The experimental evidence for these divergences has been a source of some controversy. It is debated if the accuracy of existing measurements suffices to observed the effect, or, alternatively, whether the asymptotic region where the description presented here is valid is too close to the edges of the spectrum.

REFERENCES

1. Anderson P.W.,*Phys. Rev.*,**164**, 352 (1967).
2. Mahan G.D.,*Many-Particle Physics*, Plenum (New York) 1991.
3. Nozières P. and de Dominicis C.T., *Phys. Rev.*, **178**, 1097 (1969).

II THE DISSIPATIVE TWO LEVEL SYSTEM

Introduction

The next level of complexity is given by a quantum two level system (TLS) interacting with a continuum. In the previous chapter, the local potential which was switched on had no internal dynamics of its own. A TLS is defined in a very restricted Hilbert space, built up of only two states. The only possible internal dynamics is switching between these states.

TLS's are frequently found in nature. In the simplest cases, the system has a degree of freedom which can take only two values, e.g. a fermion with spin 1/2. In a more common situation, a system, e.g an atom, is placed in a two well potential, see Fig. 6. Let us first assume that there is no tunneling between the wells. As we are interested in the low temperature behavior, each well can be, to a good approximation, described by an harmonic oscillator with frequencies ω_L, ω_R for the left and right well. For sufficiently large barriers, the only correction to this picture is given by a weak hybridization between the ground states of these oscillators, induced by quantum tunneling. The states having higher energies can be ignored. The system will be effectively restricted to the two-dimensional Hilbert space spanned by these two ground states. These systems are usually called truncated TLS. It is useful to think in the position of the atom in one well or the other as an Ising spin variable. The spin is flipped by tunneling processes.

In what follows we will first present the Hamiltonian for the TLS and its coupling to the environment. Then we will make a perturbative expansion on the coupling constant of the bosonized Hamiltonian. This coupling has consequences on the physical properties that will be presented thereafter. To finish the statistical properties will be obtained from the partition function calculated in terms of path integrals.

The TLS Hamiltonian

In the absence of interactions the Hamiltonian is

$$H_0 = t\sigma_x + \varepsilon\sigma_z \tag{35}$$

being σ_x, σ_z the Pauli matrices, t the tunneling matrix element and ε is the difference in the ground state energies of the states localized in the two wells in the absence of tunneling. Notice that due to the hopping term the two groundstates of each wells are not eigenstates of the whole system. In the following discussion we will assume that the two wells are initially degenerate, i.e. $\varepsilon = 0$.

If an atom is placed in a metal, it is going to interact with the low energy excitations of the environment. In a realistic case, the atom is coupled both to the acoustic phonons and the conduction electrons. Since the coupling to phonons scales is ω^2, it can, at low energies, be neglected with respect to the coupling to

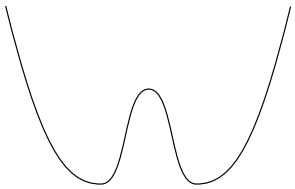

FIGURE 6. Scheme of a two well potential.

electron-hole excitation, because, as we will see later, the coupling squared has an ω dependence [1]. The most general Hamiltonian which takes this interaction into account is

$$H = H_0 + \sum_k \epsilon_k c^\dagger_{k\sigma} c_{k\sigma} + \sum_{kk'} c^\dagger_{k\sigma} [V^x_{kk'}\sigma_x + V^y_{kk'}\sigma_y + V^z_{kk'}\sigma_z] c_{k'\sigma} \tag{36}$$

Here $c^\dagger_{k\sigma}$ creates an electron with momentum k and Pauli spin σ. The first term describes the dynamics of the TLS, the second term gives the environment, and the third is the coupling.

In most cases of interest the main coupling between the system and its environment is through a term proportional to σ_z. It implies that the environment is sensitive to the position of the particle. A coupling of this form represents the screening cloud that the conduction electrons build around the atom for a fixed position of the latter. We expect that a coupling of this form reduces the tunneling, since now the atom has to carry the screening cloud when it tunnels. As we know from the previous chapter, due to the orthogonality catastrophe this screening cloud consists of an infinite number of electron-hole excitations. This interaction tends to localize the atom in a well. We can also consider the problem from a different viewpoint. The sensivity to the position of the atom which displays this coupling term can be interpreted as if the position is measured [2]. As we know, any measurement process leads to the destruction of phase coherence and to the localization of the system in a state.

Couplings of the form σ_y or σ_x are also possible. However for most problems of interest such couplings are negligible. The reason is that σ_x and σ_y have only nondiagonal matrix elements in the basis we have chosen, so any interaction proportional to them must also be proportional to the overlap of the basis states, which is of the order of the tunneling matrix element. When taken into account, these couplings describe the so-called *electron assisted tunneling*. In this process an electron is scattered by the atom while it jumps from one minimum to another.

Thus we consider the Hamiltonian:

$$H = \sum_k \epsilon_k c^\dagger_{k\sigma} c_{k\sigma} + t\sigma_x + \frac{V}{N}\sigma_z \sum_{kk'} c^\dagger_k c_{k'} \tag{37}$$

Bosonization and perturbative approach

As explained in the previous chapter, the environment can be also described in terms of quantum oscillators, which mimic the response of the electron hole pairs. Then, the Hamiltonian can be rewritten as [3]:

$$H_{TLS} = \sum_n^N n\Delta b_n^\dagger b_n + t\sigma_x + \frac{V}{N}\sigma_z \sum_n^N \sqrt{n}(b_n^\dagger + b_n) \tag{38}$$

The energy of the oscillators is bound by an upper cutoff $W = \Delta N$ of the order of the bandwidth, which is the characteristic scale with physical meaning. The type of coupling chosen $\sim \sqrt{n}$, where n refers to the energy of the oscillator, is suitable to describe the response of electron hole excitations in a metal, when a constant density of states is assumed. This assumption is valid at low energies for the most of the metals [1]. Notice that to achieve that the oscillators do not excite the atom to higher levels of the two well potential, the energy cutoff W has to be lower than the characteristic energies of each well $\hbar\omega_L, \hbar\omega_R$. It has been shown [4] that the effect of oscillators of frequency larger than ω_L, ω_R is to renormalize the tunneling matrix element. Then our assumption for the energy cutoff is always valid if we include the appropriate tunneling value.

When the TLS is frozen into one of the states of the basis (in the spin description this is equivalent to have a well defined projection of the spin) the oscillators experience a potential proportional to $\pm V/N$. Then the two positions of the TLS define two alternative equilibrium configurations for the oscillators. These two states are orthogonal. That is easy to proof. The tunneling process is equivalent to switch on a perturbation of the form

$$\pm\frac{2V}{N} \sum_n^N \sqrt{n}(b_n^\dagger + b_n) \tag{39}$$

and in the previous chapter we have seen that this potential gives rise to the orthogonality catastrophe. As a result, we cannot treat this term perturbatively. In order to do perturbation theory, we will assume that the hopping term is small related to the bandwidth $t \ll W$, then the high energy oscillators are much faster than the TLS. The nature of the ground state of (38) can be inferred from a scaling procedure. Let us consider the effect of the high energy oscillators *only*. As they are much faster than the tunneling processes, they will follow quasi instantaneously the fluctuations of the TLS. We consider the oscillators in the range $N - \delta N < n < N$, and treat the coupling term due to these oscillators to first order in perturbation theory[6]. Up to this order, the energy does not change, but the lowest states become

[6] As we have only considered a few oscillators, and not the whole set, perturbation theory is allowed. Unperturbed and perturbed states are orthogonal only in the thermodynamic limit.

$$|\uparrow\rangle \mid 0\rangle \longrightarrow |\uparrow\rangle_{dress} = |\uparrow\rangle \mid 0\rangle + \sum_{n=N-\delta N}^{N} \frac{\frac{V}{n}\sqrt{n}}{n\Delta} |\uparrow\rangle \mid n\rangle \tag{40}$$

$$|\downarrow\rangle \mid 0\rangle \longrightarrow |\downarrow\rangle_{dress} = |\downarrow\rangle \mid 0\rangle - \sum_{n=N-\delta N}^{N} \frac{\frac{V}{n}\sqrt{n}}{n\Delta} |\downarrow\rangle \mid n\rangle \tag{41}$$

The dressing of the TLS by the oscillators leads to an effective reduction in the tunneling amplitude of the TLS

$$t' = \langle\uparrow| H_{TLS} |\downarrow\rangle_{(dress)} = t(1 - \sum_{n=N-\delta N}^{N} \frac{V^2}{N^2\Delta^2}\frac{1}{n})(1 + \sum_{n=N-\delta N}^{N} \frac{V^2}{N^2\Delta^2}\frac{1}{n})^{-1} \tag{42}$$

Where the last factor is written to ensure the normalization of the groundstates. Doing a Taylor expansion in the denominator and substituting the sum by its approximate value

$$\sum_{n=N-\delta N}^{N} \frac{1}{n} \approx \frac{\delta N}{N} \tag{43}$$

the new hopping matrix element becomes

$$t' \approx t(1 - 2\frac{V^2}{W^2}\frac{\delta N}{N}) \tag{44}$$

Once the high energy oscillators have been summed, we have an effective problem with a reduced cutoff $W' = \Delta(N - \delta N)$, and a new hopping t'. But the real magnitude of interest is the ratio between these two quantities. It evolves as

$$\frac{t'}{W'} \approx \frac{t}{W}\frac{1 - 2\frac{V^2}{W^2}\frac{\delta N}{N}}{1 - \frac{\delta N}{N}} \tag{45}$$

$$\frac{t'}{W'} \approx \frac{t}{W}(1 + \frac{\delta N}{N}(1 - 2\frac{V^2}{W^2})) \tag{46}$$

It follows that if $T = 0$ and $2\frac{V^2}{W^2} > 1$, this scale flows to zero and we can proceed scaling down to $W = 0$. At this point, we have removed all the oscillators. The effective tunneling of the TLS is zero. The ground state is degenerate. The wavefunctions are those of a localized TLS, with the oscillator degrees of freedom fully relaxed to the position of the TLS, where the particle is localized. As we will see, if the temperature is not zero we have to stop the renormalization flow when the renormalized bandwidth is of the order of the thermal energy. Then some phonons (oscillators) are excited and the system is not localized.

However if $2\frac{V^2}{W^2} < 1$, $\frac{t'}{W'}$ grows. Then our approximation breaks down when the hopping and the phonon cutoff are comparable, $t' \sim W'$, because beyond this point

the assumption than the oscillators follow instantaneously the fluctuations of the TLS is no longer valid. Only oscillators with large energy can be integrated in this way, renormalizing the effective hopping element. The effective value can be obtained by integrating the flux equations. Let us define $\tilde{t}$ as $\frac{t}{W}$ and $\alpha = 2(\frac{V}{W})^2$. Then as $\tilde{t}' = \tilde{t} + d\tilde{t}$ and $W' = W + dW$, (46) can be rewritten

$$-W\frac{d\tilde{t}}{dW} = \tilde{t}(1-\alpha) \tag{47}$$

which can be straightforwardly integrated

$$\frac{\tilde{t}_W}{\tilde{t}_{W_0}} = (\frac{W_0}{W})^{1-\alpha} \tag{48}$$

or equivalently

$$\tilde{t}_W = (\frac{t_0}{W_0})(\frac{W_0}{W})^{1-\alpha} \tag{49}$$

If α is lower than unity, the flow stops when $\tilde{t} \approx 1$ or $t_{ren} \approx W_{ren}$; from (49), t_{ren} satisfies

$$t_{ren} = W_{ren} = t_0(\frac{t_0}{W_0})^{\frac{\alpha}{1-\alpha}} \tag{50}$$

Indeed the phonons have reduced $t_0 \to t_{ren}$. This is the only energy scale that survives in the problem. Above this scale, all the oscillators have been integrated, contributing to renormalize t. Below this scale, there exist low energy oscillators, but we can assume that the TLS is fluctuating much faster than the typical frequencies of these oscillators. On the time scale at which the oscillators can respond, the coupling can be neglected. Thus, the picture which emerges is that of a TLS oscillating at a renormalized tunneling rate. The oscillators which are much faster than this rate follow instantaneously the TLS. The low energy oscillators are decoupled from the TLS.

If the temperature is not zero, the flow stops at $W = T$ for $\alpha > 1$ and for $\alpha < 1$ at $max\{T, W_t\}$ where W_t satisfies (50). Suppose that it stops at $W = T$, then

$$t_{ren}(T) = t_0(\frac{T}{W_0})^{\alpha} \tag{51}$$

We recover the known result that at $T = 0$ and $\alpha > 1$, $t_{ren} = 0$ [7]. For finite temperature or $\alpha < 1$, there is a crossover between a high energy, high temperature regime, and a low energy, low temperature regime. Note that, at low temperatures, the dynamics of the low energy modes are governed by thermal fluctuations. Hence, they are effectively decoupled from the two level system, and play no role in the response of the system.

---

[7] Obviously, if $T = 0$ and $\alpha < 1$, the flow does not stop at $W = T$, but at $W = W_t$

Physical properties

Now we study the effect that the coupling to the oscillators has on different physical properties of the TLS. Because of the discreteness of the system, physical operators can be written in terms of 2×2 Pauli matrices.

$\sigma_z(t)$ is the operator which measures the position of the particle at time t. σ_z is 1 if the particle is in the right well and -1 if it is in the left one. Its mean value $\langle \sigma_z \rangle$ is zero if $\alpha < \alpha_c$, because tunneling between the two wells is allowed. On the contrary, $\langle \sigma_z \rangle \neq 0$ for $\alpha > \alpha_c$, as the coupling to the oscillators has renormalized the tunneling down to zero. The two level system self-traps at $T = 0$. Now, in the same way, $\langle \sigma_x \rangle$ measures how much the particle fluctuates between the two wells. It is given by

$$\langle \sigma_x \rangle = \frac{\partial E}{\partial t} \tag{52}$$

As seen before, if $\alpha < \alpha_c$, we cannot proceed the scaling beyond t_{ren}, given by (50). The oscillators which remain satisfy $\omega_n < t_{ren}$, then to first approximation $H_{eff} = t_{ren}\sigma_x$ and the energy of the ground state

$$E = -t_{ren} = t_0 (\frac{t_0}{W_0})^{\frac{\alpha}{1-\alpha}} \tag{53}$$

From here

$$\langle \sigma_x \rangle = \frac{1}{1-\alpha} (\frac{t_0}{W_0})^{\frac{\alpha}{1-\alpha}} \tag{54}$$

We can also study measurable properties such as the specific heat and the magnetic susceptibility. We assume $\alpha < 1$ and start from (38) with the hopping element given by (50). As the high energy oscillators have been eliminated in the renormalization process, it seems to be reasonable to consider in first approximation that the remaining oscillators, with a frequency supposed to be much lower than the hopping matrix element, are decoupled from the TLS. The Hamiltonian would be

$$H^0 = \sum_n \Delta n b_n^\dagger b_n + t_{ren}\sigma_x \tag{55}$$

which ground state is the antisimetric combination

$$\mid \varphi \rangle^0 = \frac{1}{\sqrt{2}} (\mid \uparrow \rangle - \mid \downarrow \rangle) \mid 0 \rangle \tag{56}$$

Its excitation spectrum is shown if Fig. 7. The low energy modes are obtained, from the ground state, exciting oscillators

$$\mid \varphi_n^{LOW} \rangle^0 = \frac{1}{\sqrt{2}} (\mid \uparrow \rangle - \mid \downarrow \rangle) \mid n \rangle \tag{57}$$

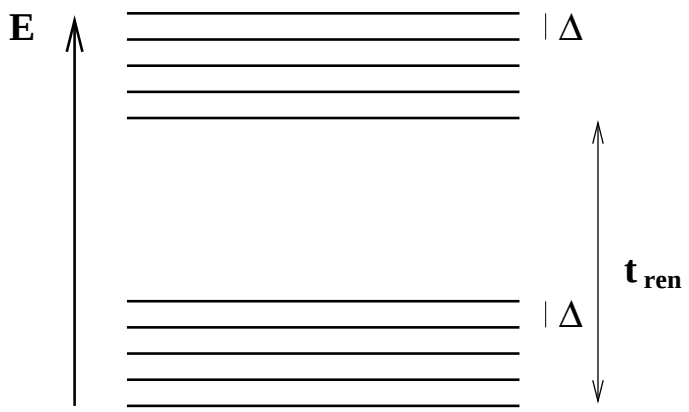

FIGURE 7. Excitation spectrum associated to the ground state of the Hamiltonian (55).

while the high energy band, starts from the simetric combination of the states $|\uparrow\rangle$ and $|\downarrow\rangle$.

$$\mid \varphi_n^{HIGH}\rangle^0 = \frac{1}{\sqrt{2}}(|\uparrow\rangle + |\downarrow\rangle) \mid n\rangle \tag{58}$$

Each band has a constant density of states with spacing between levels Δ. We include perturbatively the coupling, assuming now that we only have low energy oscillators, as compared to the renormalized tunneling matrix element. Perturbation theory is justified, as the operator σ_z only mixes low energy states with states at energies much higher than those of the fastest oscillators.

$$\frac{V}{N}\sigma_z \sum_n \sqrt{n}(b_n^\dagger + b_n) \tag{59}$$

between the TLS and the oscillators. To first order the eigenstates become

$$\mid \varphi_p^{(1)}\rangle = \mid \varphi_p\rangle + \sum_n \frac{\langle \varphi_n \mid \frac{V}{N}\sigma_z \sum_n \sqrt{n}(b_n^\dagger + b_n) \mid \varphi_p\rangle}{E_P^0 - E_n^0} \mid \varphi_n\rangle \tag{60}$$

From here, it is evident that only excitations of the high energy band will contribute to the modification of the groundstate wave function.

$$\mid \varphi_0^{(1)}\rangle = \frac{1}{\sqrt{2}}(|\uparrow\rangle - |\downarrow\rangle) \mid 0\rangle + \sum_n \frac{V\sqrt{n}}{N(t_{ren} + \omega_n)}(|\uparrow\rangle + |\downarrow\rangle) \mid n\rangle \tag{61}$$

while the low energy excited states

$$\mid \varphi_n^{LOW(1)}\rangle = \frac{1}{\sqrt{2}}(|\uparrow\rangle - |\downarrow\rangle) \mid n\rangle + \frac{V\sqrt{n}}{N(t_{ren} + \omega_n)}(|\uparrow\rangle + |\downarrow\rangle) \mid 0\rangle \tag{62}$$

The correction to the energy is zero at first order in perturbation theory, but at second order

$$\varepsilon_n^{(2)} = \sum_{p \neq n} \frac{\mid \langle \varphi_n \mid \frac{V}{N}\sigma_z \sum_n \sqrt{n}(b_n^\dagger + b_n) \mid \varphi_p \rangle \mid^2}{E_P^0 - E_n^0} \tag{63}$$

$$\varepsilon_n^{(2)} = \frac{V^2 n}{N^2(t_{ren} + \omega_n)} \simeq \frac{n\Delta V^2}{NWt_{ren}} \tag{64}$$

The correction due to an impurity to the energy of a bulk system is of the form $1/N$, smaller as the size of the system increases. The effect is more important in the states with high energy. The energy of the nth eigenstate is

$$\epsilon_n = n\Delta(1 - \frac{V^2}{NWt_{ren}}) \tag{65}$$

The new spectrum has also a constant density of states but the level spacing is smaller

$$\Delta \longrightarrow \Delta(1 - \frac{V^2}{NWt_{ren}}) \tag{66}$$

This fact has important consequences in physical properties such as the specific heat. A system which spectrum presents a constant density of states, has a specific heat of the form

$$C \sim \frac{T}{\Delta} \tag{67}$$

Then, the inclusion of the coupling to the oscillators modify it

$$\frac{T}{\Delta} \longrightarrow \frac{T}{\Delta(1 - \frac{V^2}{NWt_{ren}})} \sim \frac{T}{\Delta}(1 + \frac{V^2}{NWt_{ren}}) \tag{68}$$

As $t_{ren} \ll W$, the contribution of the perturbation is very large. In the next chapter, the Kondo problem, the effect of a magnetic impurity in a metal will be explained in terms of a dissipative TLS [3–6]. These impurities will increase a great deal the specific heat. In particular, if N_{imp} is the number of impurities, the specific heat will be

$$C \sim \frac{T}{\Delta}(1 + \frac{V^2 N_{imp}}{NWt_{ren}}) \tag{69}$$

The dynamics of the TLS is given by the correlation function $P(t) = \langle \sigma_z(t)\sigma_z(0) \rangle$. P(t) allow us to know where is the particle at time t. We will assume that it starts in the right well, $P(0) = 1$. If there is no dissipation the particle oscillates between the two wells, $P(t) = \cos 2t_0 t$ and as $t \to \infty$, $\langle \sigma_z \rangle \to 0$. The environment suppresses quantum coherence, which is the origin of these oscillations. Hence, we expect $P(t) \to 0$ as $t \to \infty$. The decay of $P(t)$ can still show damped oscillations, or be completely incoherent.

We consider the Fourier transform of $P(t)$ or response function

$$\chi(\omega) = \sum_{\omega} \mid \langle 0 \mid \sigma_z \mid n \rangle \mid^2 \delta(\omega - \omega_n) \tag{70}$$

As

$$\mid \langle 0 \mid \sigma_z \mid n \rangle \mid^2 = (\frac{V\sqrt{n}}{N t_{ren}})^2 = \frac{V^2 \omega_n}{NW t_{ren}^2} \tag{71}$$

the response function is linear in ω

$$\chi(\omega) \sim \frac{\alpha}{t_{ren}^2} \omega \tag{72}$$

Then

$$P(t) \sim \frac{\alpha}{(t_{ren} t)^2} \tag{73}$$

and relaxation is incoherent. Later we will see that there is other fixed point at $\alpha = 1/2$. The previous equations for $P(t)$ are valid for α close to unity. For $0 < \alpha < 1/2$ there are damped oscillations. They can only be obtained by numerical methods [7].

We can also obtain the magnetic susceptibility

$$Re\chi(\omega = 0) = \int_0^{t_{ren}} \frac{\chi(\omega)}{\omega} d\omega = \frac{V^2}{NW t_{ren}} \tag{74}$$

Here we recover the same contribution we found in the specific heat. So we can define an universal quantity, called the Wilson ratio as

$$\frac{C}{\chi T} \tag{75}$$

An universal Wilson ratio is characteristic of fermionic systems [8].

Mapping onto the resonant level model

Let us consider another way of doing all calculations. In the previous chapter, devoted to the orthogonality catastrophe, we found a canonical transformation which allowed us to write the dissipative Hamiltonian in the form of a sum of oscillators and to relate both ground states. That transformation can be generalized to the present case, including the Pauli matrices associated to the TLS. We define [3]

$$U = exp[-\sum_n \frac{V\sigma_z}{N\Delta\sqrt{n}}(b_n^\dagger - b_n)] \tag{76}$$

It leads to bosonic operators $\tilde{b}_n^\dagger$ which satisfy

$$b_n^\dagger = \tilde{b}_n^\dagger - \frac{V}{N}\frac{\sigma_z}{\sqrt{n}\Delta} \tag{77}$$

It is then straightforward to rewrite

$$\sum_n \Delta n b_n^\dagger b_n + \frac{V\sigma_z}{N}\sum_n \sqrt{n}(b_n^\dagger + b_n) \longrightarrow \sum_n \Delta n \tilde{b}_n^\dagger \tilde{b}_n \tag{78}$$

Consider now the hopping term. To treat it, it is useful to decompose σ_x in terms of σ_+ and σ_- which satisfy:

$$\sigma_+ \, |\uparrow\rangle = 0 \tag{79}$$
$$\sigma_- \, |\downarrow\rangle = 0 \tag{80}$$

where as usual the state $|\uparrow\rangle$ refers to the right well and $|\downarrow\rangle$ to the left one. Then σ_+ plays a role only if the TLS is in the $|\downarrow\rangle$ position and σ_- only if it is in the $|\uparrow\rangle$ position.

These operators transform according to

$$U^\dagger t\sigma_+ U = texp(\sum_n \frac{2V}{W\Delta\sqrt{n}}(\tilde{b}_n^\dagger - \tilde{b}_n)) \tag{81}$$
$$U^\dagger t\sigma_- U = texp(-\sum_n \frac{2V}{W\Delta\sqrt{n}}(\tilde{b}_n^\dagger - \tilde{b}_n)) \tag{82}$$

And the TLS Hamiltonian becomes

$$\begin{aligned} H_{TLS} = {} & t\sigma_+ exp(\sum_n \frac{2V}{W\Delta\sqrt{n}}(\tilde{b}_n^\dagger - \tilde{b}_n)) + \\ & + t\sigma_- exp(-\sum_n \frac{2V}{W\Delta\sqrt{n}}(\tilde{b}_n^\dagger - \tilde{b}_n)) + \sum_n \omega_n \tilde{b}_n^\dagger \tilde{b}_n \end{aligned} \tag{83}$$

This way of writing the Hamiltonian of the TLS is better for a rigorous field theoretical analysis, as we can study it up to 3rd or 4th order in a systematic way. To do it we identify $\tilde{b}_n^\dagger \equiv \phi_k^\dagger$ and

$$\phi^\dagger \equiv exp(-\sum_n \frac{2V}{W\Delta\sqrt{n}}(\tilde{b}_n^\dagger - \tilde{b}_n)) \tag{84}$$
$$\phi \equiv exp(\sum_n \frac{2V}{W\Delta\sqrt{n}}(\tilde{b}_n^\dagger - \tilde{b}_n)) \tag{85}$$

and compare the resulting Hamiltonian

$$H_{TLS} = t(\sigma_+\phi + \sigma_-\phi^\dagger) + \sum_k \epsilon_k \phi_k^\dagger \phi_k \tag{86}$$

with the resonant level model Hamiltonian [9]

$$H_{RL} = t(d^\dagger \phi + d\phi^\dagger) + \sum \epsilon_k \phi_k^\dagger \phi_k \tag{87}$$

which describes the interaction between an impurity and a band of spinless fermions. Using

$$\sigma_+ \longleftrightarrow d^\dagger \tag{88}$$

$$\sigma_- \longleftrightarrow d \tag{89}$$

we find

$$\sigma_z = 2\sigma_+\sigma_- - 1 = 2d^\dagger d - 1 \tag{90}$$

and the TLS is mapped onto the resonant level model which is an exactly soluble problem.

PATH INTEGRAL APPROACH

Introduction

Statistical properties can be obtained from the partition function. It also contains information about the spectrum of the Hamiltonian. The partition function can be written in terms of an imaginary time path integral. In particular, for open quantum systems it is more suitable, if possible, to integrate out the environmental degrees of freedom and to work with the reduced partition function,

$$Z^{red} = \int Dq(\tau) exp(S_{eff}^E[q(\tau)]/\hbar) \tag{91}$$

Here $q(\tau)$ denotes the possible paths of the particle. At finite temperature, the path sum is over all periodic paths $q(\tau) = q(\tau + \hbar\beta)$ and β is, as usual related to the temperature by [8] $\beta = 1/T$. The effective, Euclidean action, takes into account the effect of the coupling to the environmental modes. $S_{eff}^E[q]$ determines the path probability in the integral expression for the partition function.

In the semiclassical limit, the functional integral is dominated by the paths where $S_{eff}^E[q]$ is minimum, namely by the classical paths. As the motion is in imaginary time, the sign of the potential term is reversed. In an inverted double well, the only classical paths available at low temperatures, apart from the static path involving zero kinetic energy and the particle localized in one of the minimum of the not-reversed potential, are those which are built up by well separated instantons or kinks [10], see Figure 8. These are the paths that interpolate at times $-\infty$ and $+\infty$ between the two distinct ground states. In a tight binding limit, we can assume

---

[8] In units of the Boltzmann constant K_B, which is omitted through the text

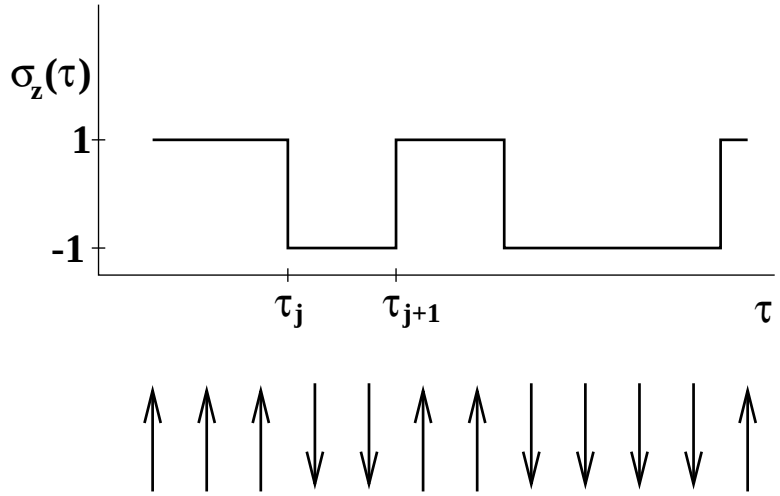

FIGURE 8. Kinks in a one dimensional Ising model.

that the particle stays most of the time at the center of the wells with sudden and instantaneous tunnel events (or spin flips in the Ising notation). Each kink is followed by an antikink. This picture is specially useful because, as we will see, the environmental influence can be expressed in terms of kink interactions. We will map the dissipative TLS onto an effective unidimensional Ising model [3,11–13].

Partition function

Let us start from the Hamiltonian (38). We want to calculate the partition function

$$Z = \sum_n \langle n \mid e^{-\beta H} \mid n \rangle \tag{92}$$

where $\mid n\rangle$ labels each eigenstate with well defined positions for the particle and the oscillators. As usual in path integral approaches, we make an analytic continuation $t \to -i\tau$.

To facilitate the integration of the oscillators, we substitute

$$x_n = \frac{1}{\sqrt{2n\Delta}}(b_n^\dagger + b_n) \tag{93}$$

Then

$$Z \sim \int dq(\tau) e^{-S^E[q]} \prod_m \int dx_m(t) e^{-\int d\tau [\frac{m}{2}(\dot{x}_m^2 - \omega_0^2 x_m^2) - \frac{V}{N}\sigma_z(\tau) n\sqrt{2\Delta} x_n]} \tag{94}$$

Here the $S^E[q]$ is the Euclidean action for the particle without taking into account the oscillators and integrals in τ go from 0 to $\beta\hbar$. From the oscillators point of

view, the integrals are gaussians. To solve them, we consider the Fourier transform of $x_n(\tau)$

$$x_\omega^n = \frac{1}{\sqrt{2n}} \int x_n(\tau) e^{i\omega\tau} \tag{95}$$

Each integral can be written on the form

$$\int dx(\tau) e^{\int d\omega \frac{\omega^2+(n\Delta)^2}{2} (x_\omega + \int d\tau \frac{V}{N} \frac{\sigma_z(\tau)\sqrt{2\Delta} n e^{i\omega\tau}}{\omega^2+(n\Delta)^2})^2} e^{-\int d\tau d\tau' d\omega \sigma_z(\tau)\sigma_z(\tau') \frac{V^2}{N^2} \frac{n^2\Delta e^{i\omega(\tau-\tau')}}{\omega^2+(n\Delta)^2}} \tag{96}$$

with a redefinition of the integral variable [9] we can perform the integral. We have then an effective problem which depends on $\sigma_z(\tau)$. $\sigma_z(\tau)$ does not depend explicitly on the oscillators but on the particular path followed by the TLS. Taking into account all the oscillators, the last factor in (96) expresses an interaction between kinks

$$e^{-\int d\tau d\tau' J(\tau,\tau')\sigma_z(\tau)\sigma_z(\tau')} \tag{97}$$

with

$$J(\tau,\tau') = \sum_n \int d\omega \frac{V^2}{N^2} \frac{n^2\Delta e^{i\omega(\tau-\tau')}}{\omega^2 + n^2\Delta^2} \tag{98}$$

Performing the integral in frequencies

$$J(\tau,\tau') = \sum_n \frac{V^2}{N^2} n e^{-n\Delta(\tau-\tau')} \tag{99}$$

$J(\tau,\tau')$ only depends on $\tau - \tau'$ so, in what follows, it will be denoted by τ and

$$J(\tau) = \frac{V^2}{N^2} \frac{\partial}{\partial(\Delta\tau)} [-\frac{1}{1-e^{-\Delta\tau}}] = \frac{V^2}{N^2} \frac{e^{-\Delta\tau}}{(1-e^{-\Delta\tau})^2} \tag{100}$$

We have a long-range effective interaction between the kinks. However it decays with distance. In the thermodynamic limit we can expand the exponential and $J(\tau)$ becomes

$$J(\tau) \sim \frac{V^2}{W^2\tau^2} \tag{101}$$

This interaction can be compared with a one dimensional Ising model

$$H = \sum_{n,n'} J_{n,n'} S_n S_{n'} \tag{102}$$

---

[9] This redefinition is carefully explained in the chapter devoted to system plus environment models.

As we see, our problem is formally identical to a one dimensional Ising model with long range interaction, such that the interaction between the binary variables has a τ^{-2} dependence. The partition function of the whole system becomes

$$Z \sim \ e^{-S^E[q]} e^{-\int d\tau d\tau' \sigma_z(\tau)\sigma_z(\tau') \frac{V^2}{W^2\tau^2}} \tag{103}$$

The presence of the environmental coupling has introduced interactions between the kinks. In the low temperature limit, after two integrations by parts, the exponent due to interactions in (103) acquires the form [11,12]

$$(\frac{V}{W})^2 \int\int d\tau d\tau' (\frac{d\sigma}{d\tau})(\frac{d\sigma}{d\tau'} ln(\frac{\mid \tau - \tau' \mid}{\tau_c})) \tag{104}$$

It becomes clear that the kinks interact logarithmically due to the hopping from one place to another (notice the factors $d\sigma/d\tau$) and that this damping term is a nonlocal "kinetic energy " contribution.

In the kink approximation

$$\frac{d\sigma}{d\tau} = 2\sum_i \epsilon_i \delta(\tau - \tau_i) \tag{105}$$

where $\epsilon_i = \pm 1$ depending if it corresponds to a kink or an antikink situated at τ_i. The delta function in (105) strictly has a finite width τ_c which reflects that the path cannot change on a scale smaller than the kink width. The logarithmic interaction is cut off at the same scale, since distinct kinks are not well defined if their separation is less than their width. Then, in the kink approximation this exponent is given by

$$4(\frac{V}{W})^2 \sum_{ij} \int\int \frac{d\tau_i}{\tau_c}\frac{d\tau_j}{\tau_c} \epsilon_i\epsilon_j ln \mid \frac{\tau_i - \tau_j}{\tau_c} \mid \tag{106}$$

the short time cutoff out of the logarithm appears due to the finite width of the delta function, and the partition function

$$Z = \sum_{n=0}^{\infty} \tilde{t}^{2n} \int \frac{d\tau_{2n}}{\tau_c} ... \int \frac{d\tau_1}{\tau_c} exp\{K \sum_{i>j} \epsilon_i\epsilon_j ln \mid \frac{\tau_i - \tau_j}{\tau_c} \mid\} \tag{107}$$

where $\tilde{t} = t\tau_c$ (or $t\omega_c$ as denoted previously) is called the *fugacity*. Here we have taken into account only contributions which give periodic paths[10]. Small fugacity implies a dilute gas or a small mean tunneling rates. K can be interpreted [11] as the inverse temperature of the gas of kinks interacting via the logarithmic potential; this temperature has to be distinguished from the real temperature which gives up the extent of the spatial dimension in imaginary time.

Another interpretation is also possible as the exponential can be rewritten as

---

[10] This is reflected in the exponent of the fugacity.

$$\exp(\sum_{i>j}\int\int d\tau_i d\tau_j ln \mid \frac{\tau_i-\tau_j}{\tau_c} \mid^{q_i q_j}) \tag{108}$$

Then the gas of kinks is equivalent to a gas of charges [15], with $q_i = \pm 2(\frac{V}{W})$ which interact logarithmically. The total charge is zero $Q = \sum_i q_i = 0$. As the effective interaction decays with the distance (in imaginary time) between them, if they were far enough, namely, if our gas of kinks is sufficiently dilute, we can ignore these interactions. With this idea in mind, we will try to replace our problem by one with a longer cutoff.

$$\tau_c \longrightarrow \tau_c' = \tau_c e^{\delta} \tag{109}$$

Let us first see the effect from a dimensional point of view. In the expression of the partition function the short time cutoff appears in power form

$$\tau_c^{-2n}\tau_c^{-\sum_{i>j} q_i q_j} \tag{110}$$

Replacing the cutoff by a longer (in time) one

$$\tau_c^{-2n}\tau_c^{-\sum q_i q_j} \longrightarrow \tau_c'^{-2n}\tau_c'^{-\sum q_i q_j} e^{2n\delta} e^{\delta \sum q_i q_j} \tag{111}$$

The exponential factors tell us if the interaction between kinks grows or decreases upon increasing the cutoff. We rewrite them

$$e^{2n\delta} e^{\delta \sum_{i>j} q_i q_j} = e^{2n\delta} e^{\delta(\frac{Q^2}{2} - \sum \frac{q_i^2}{2})} \tag{112}$$

We can do this because the total charge is zero. The exponential factor is

$$e^{\delta 2n(1-\frac{q^2}{2})} \tag{113}$$

with $q^2 = 4(\frac{V}{W})^2$. Notice $\alpha = \frac{q^2}{2}$.
This factor can be included in the definition of the fugacity

$$\tilde{t} \longrightarrow \tilde{t}' = \tilde{t} e^{\delta(1-\frac{q^2}{2})} \tag{114}$$

After the scaling process, the gas of kinks is coarse-grain and kinks which are very close ($\tau_c < \delta\tau < \tau_c'$) are invisible, that is, cannot be resolved. In the same process the hopping and the Ising interaction also change, the latter due to the renormalization of the charges and cutoff.

From a formal point of view, the scaling equations can be derived from (107) by integrating out the close pairs of charges of separation between τ and $\tau' = \tau + d\tau$ and incorporating this effect into a new α and $\tilde{t}$. From the naive calculations done at the beginning of the chapter we found that for a weak enough coupling the particle tunnels back and forth between the two wells and quickly loses memory of the well

where it was initially. This is no longer true if the coupling is greater than a critical strength, then spontaneous symmetry breaking occurs leading to a localized regime signaled by a vanishing tunneling rate. Our calculations predicted that the critical coupling was $\alpha_c = 1$. We are interested in an expansion around this value. As noted before, the effective action we start from, is the same that applies in the one dimensional Ising model with τ^{-2} interactions. So we can take the renormalization group relations from the seminal work done by Kosterlitz [11,12,14]. He found

$$\frac{d\tilde{t}}{dln\tau_c} = (1-\alpha)\tilde{t} \tag{115}$$

$$\frac{d\alpha}{dln\tau_c} = -\alpha\tilde{t}^2 \tag{116}$$

This equations are valid for $\tilde{t} \ll 1$. α and $\tilde{t}$ describe entirely the dynamics of the TLS, in particular, they describe the transition line between a disordered ($\langle\sigma_z\rangle = 0$) to an ordered ($\langle\sigma_z\rangle \neq 0$) phase. This transition is of the Berezinski-Kosterlitz-Thouless type [14]. It is a continuum transition characterized by a fixed line, which is stable for $\alpha > 1$ and unstable for $\alpha < 1$, and separates an ordered phase from a disordered one. The scaling trajectories close to $\alpha = 1$ are hyperbolas determined by

$$(1-\alpha)^2 - 4\tilde{t}^2 = cte \tag{117}$$

This equation implies that the points to the left of the separatrix $\tilde{t} = \frac{1}{2}(\alpha - 1)$ in the $\tilde{t}$, α plane scale to the large $\tilde{t}$ region dominated by tunneling events. On the other hand the points to the right of this separatrix scale to $\tilde{t} = 0$. The phase transition is found at $\alpha_c = 1 + 2\frac{t_0}{\omega_0}$. From here, if $\alpha \gg 1$, we can treat it as a constant and we recover the naive equations we obtained at the beginning of the chapter. They showed that $t \longrightarrow 0$ as $T \longrightarrow 0$. This vanishing value of the tunneling rate as the temperature approaches zero is the precursor of the spontaneous symmetry breaking which takes place at $T = 0$. However for different values of α, the naive calculations neglected the variation of α and seemed to predict a vertical transition line.

Consider now the $\alpha < 1$ regime. As $\tilde{t}$ scales to large values we leave the validity of the flow equations. However, we can have further insight in its behavior thanks to the mapping onto the resonant level model, as well as the equivalence to the Kondo problem which will be studied in the next chapter.

Although the derivation of the following results is out of the scope of these notes, let us summarize the most important characteristics which appear in the strong-coupling regime [3,13] . In this region of the parameter space, the Bethe ansatz solution for the Kondo problem [16] tells us that it appears a fixed point for $t \longrightarrow \infty$ and $\alpha = 1/2$. Between $\alpha = 0$ and $\alpha = 1/2$ the behavior of the system can be obtained from the resonant level Hamiltonian [3]. Its flow is vertical, as shown in Fig. (9) where the possibility of new relevant operators appearing at intermediate values of $\tilde{t}$ is discarded.

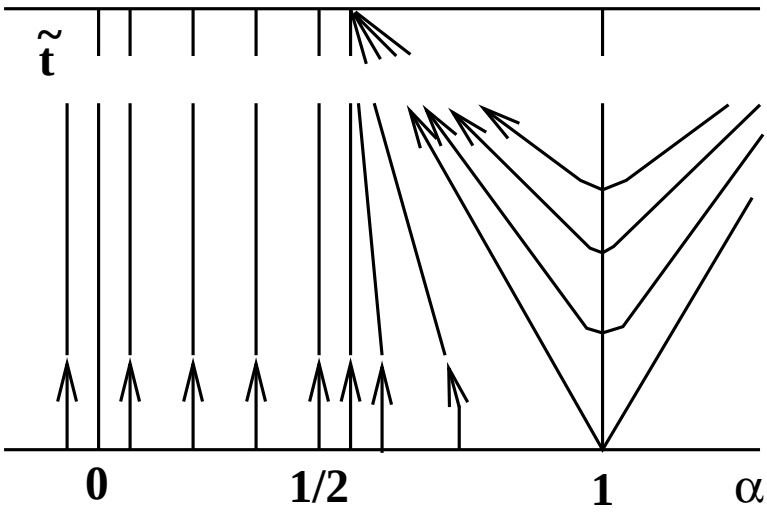

FIGURE 9. Flux diagram of the TLS.

REFERENCES

1. Guinea F., *Phys. Rev. Lett.*, **53**, 1268 (1984).
2. Hakim V. and Ambegaokar V., *Phys. Rev. A*, **32**, 423 (1985).
3. Guinea F., Hakim V. and Muramatsu A., *Phys. Rev. B*, **32**, 4410 (1985).
4. Leggett A.J., Chakravartyt S., Dorsey A.T., Fisher M. P. A., Garg A. and Zwerger W., *Rev. of Mod. Phys.*, **59**, 1-85 (1987).
5. Weiss U.,*Quantum Dissipative Systems*, World Scientific, 1993.
6. Cox D.L. and Zawadowski A., *cond-mat* 9704103. Submitted to Advances in Physics.
7. F. Guinea, Phys. Rev. B **32**, 4486 (1985).
8. Pines D. and Nozières P., *The Theory of Quantum Liquids*, Edit. W.A. Benjamin, New York 1966.
9. Tsvelick A.M. and Wiegmann P.B., *Phys. Rev. B*, **1**, 1522 (1970).
10. Callan C. G. and Coleman S., *Phys. Rev. D*, **16**, 1762 (1977).
11. Chakravarty S., *Phys. Rev. Lett.*, **49**, 681 (1982).
12. Bray A.J. and Moore M.A., *Phys. Rev. Lett.*, **49**, 1545 (1982).
13. Hakim V., Muramatsu A. and Guinea F., *Phys. Rev. B*, **30**, 464 (1984).
14. Kosterlitz J.M., *Phys. Rev. Lett.*, **37**, 1577 (1976).
15. Schmid A., *Phys. Rev. Lett.*, **51**, 1506 (1983).
16. Wiegmann P.B., *J. Phys. C*, **14**, 1463 (1981).

III THE KONDO PROBLEM

Introduction

The Kondo model describes magnetic impurities in a non magnetic metal. The changes induced by magnetic impurities in the properties of the system remained was one of the most studied problems in condensed matter physics for many years. Experimentally, it was known that the resistivity due to magnetic impurities had a significant temperature dependence [1], while the standard theory of electron impurity scattering leads to a residual resistivity which is independent of temperature at low temperatures [2]. In addition, the spin of the impurities seemed to disappear at low temperatures, as the magnetic susceptibility does not show the characteristic T^{-1} dependence of isolated moments [11]. Instead, the susceptibility tends to a constant as $T \to 0$.

A lot of effort was devoted to the comprehension of this problem, which lead to a number of surprises and important results. It became a landmark in modern condensed matter physics, as it was the first problem which showed in full the power of renormalization group ideas [3].

We will consider a single magnetic impurity weakly coupled to a band of delocalized, non interacting, conducting electrons. The problem has three energy scales: the electronic bandwidth, W, (or the density of states), the magnitude of the coupling, which we call J for the moment, and the temperature, T. Weak coupling implies that $J \ll W$. We will also assume that $T \ll W$. These inequalities are not too restrictive, as, typically, $W \sim 1\text{eV} \sim 10^4\text{K}$, and J, in most cases does not exceed 0.1eV.

We first analyze the case of an impurity with $S = 1/2$. We first present two approaches based on Renormalization Group ideas, which changed, in many respects, the tools and concepts in the theory of interacting electrons. They are complementary, and provide a fairly complete solution of the problem. Then, we discuss extensions and variations of the $S = 1/2$ Kondo model.

Kondo model for spin 1/2

The simplest version of the Kondo model [4] describes a spin 1/2 magnetic impurity in a metal. The Hamiltonian is

$$H = \sum_k \epsilon_k c_k^\dagger c_k + J \sum_{k,s,s'} \vec{S} c_{k,s}^\dagger \vec{\sigma}_{s,s'} c_{k's'} \tag{118}$$

The first term describes the metal, and the second the interactions between the spin of the impurity and the spin of the electrons. The impurity spin has no internal

[11] To obtain the susceptibility due to the impurity one has to subtract the susceptibility of the pure metal from the total susceptibility of the metal plus the impurity.

dynamics, but a spin flip can occur if the spins of the electrons also change. One might think that the nature of the Kondo problem is due to the magnetic impurity, not to the conduction band. On the contrary, the main physics is on the properties of the conduction band rather than the impurity itself. The importance of the impurity is simple: it forces one to study the conduction band as a many-electron system. This is a consequence of the spin flip scattering of the impurity and the spin conservation law.

The second term in (118) is also usually written in terms of the effective spin operator due to the conduction electrons at the impurity site. Assuming it is placed at the origin, it takes the form

$$J\vec{S}\vec{s}(0) = J\vec{S}\sum_{\sigma} c_s^\dagger(0)\vec{\sigma}_{s,s'}c_{s'}(0) \tag{119}$$

where $c_s(0) = L^{-1/2}\sum_k c_{k,s}^\dagger$.

In the genuine Kondo problem, the interaction satisfies rotational invariance but, in order to associate the Kondo with the two level system, it is useful to generalize the isotropic coupling in the original model to the case where the exchange constants J_z for the $S_z s_z$ term and $J_\perp$ for $S_x s_x + S_y s_y$ are independent parameters. The anisotropic Kondo Hamiltonian takes the form

$$H = \sum_k \epsilon_k c_k^\dagger c_k + \frac{J_z}{2}\sigma_z \sum_{s,k,k'} c_{s,k}^\dagger c_{s,k'} + J_\perp \sum_{k,k'}(\sigma_+ c_{k\uparrow}^\dagger c_{k'\downarrow} + \sigma_- c_{k\downarrow}^\dagger c_{k'\uparrow}) \tag{120}$$

with $\sigma_\pm = (\sigma_x \pm i\sigma_y)/2$. The role of the J_z term is similar to that of a static impurity, except that it couples with different sign to each spin species. Spin flip processes are described by $J_\perp$. The parameters J_z and $J_\perp$ have dimensions of energy times length, and therefore the dimensionless coupling constants are ρJ_z and $\rho J_\perp$ where ρ is the density of states at the Fermi surface per spin polarization and normalized to the volume of the unit cell occupied by the impurity.

Mapping onto the two level system

Spin flip processes are the counterpart of the tunneling events of the TLS discussed in the preceding section. When only the longitudinal coupling J_z is kept, the system is exactly soluble, and is equivalent to the dissipative TLS in the absence of the TLS dynamics. The spin has two orientations, and the conduction electrons relax to them as if an external potential acted upon them.

The mapping of the Kondo Hamiltonian onto the TLS can be made more rigorous way by noting that the electronic degrees of freedom can be integrated out, leaving an effective theory, with retarded interactions, for the impurity spin. As before, this theory is best expressed in the path integral formulation. In an analogous way to the previous chapter, the possible paths for the spin are successions of binary variables, which represent the z-component of the spin at a given instant. The

interactions induced by the integrated out conduction electrons can be written as effective couplings between the spins at different times. This was the path originally used by Yuval and Anderson [5] to tackle, successfully, the Kondo Hamiltonian . The path integral over spin histories was expressed as an integral over spin flips. The effective interaction between the spin flips depends logarithmically on their distance (in time). This is analogous to the interactions found in the TLS case. The interactions between spin flips separated by a time interval t arises from a retarded electron propagator of the type $\langle c_\uparrow^\dagger(t)c_\downarrow(t)c_\downarrow^\dagger(0)c_\uparrow(0)\rangle$. This propagator decays as t^{-2} when the electrons are in equilibrium and do not interact. Yuval and Anderson went a step further, and calculated this propagator when the equilibrium state is disturbed by the sudden change of the static potential described by the J_z term. The propagator becomes, at long times, $t^{-2-cJ_z\rho}$, where c is a constant of order unity.

Hence, we find the same kind of interaction in the TLS. The mapping is effective when we do the equivalence

$$t \sim J_\perp \rho \tag{121}$$

$$\frac{V}{W} \sim J_z\rho + 1 \tag{122}$$

From the above equivalence it is evident that we get an analogous renormalization flux diagram (see previous section), although now it is shifted; see Fig. 10. The renormalization flows isotropically only in the case when the bare coupling constants are isotropic. If this is not the case, but the parallel coupling J_z is ferromagnetic, we can, at low temperatures, neglect spin flip processes. But if the coupling is antiferromagnetic, $J_\perp$ flows upwards. It reflects the tendency of the system to form a singlet. The scaling equations analogous to those in the TLS case can also be derived from a diagrammatic analysis. They read [6]:

$$\frac{dJ}{d(lnW)} = -\rho J^2 \tag{123}$$

$$J_{eff} = \frac{J_0}{1 - J_0\rho ln\frac{W_0}{W}} \tag{124}$$

for the isotropic case, and

$$\frac{dJ_\perp}{dlnW} = -\rho J_\perp J_z \tag{125}$$

$$\frac{dJ_z}{dlnW} = -\rho J_\perp^2 \tag{126}$$

subject to $J_\perp^2 - J_z^2 = cte$, for the anisotropic case. If $J_(0) < 0$ (ferromagnetic case) $J_{eff} \to 0$ in the renormalization procedure but if $J_(0) > 0$ (antiferromagnetic case) J_{eff} diverges at $W \sim T_k \sim W_0 e^{-\frac{1}{\rho J_0}}$. Then the singlet will be formed if the temperature satisfies $T < T_K$. As the electron is trapped, the site of the

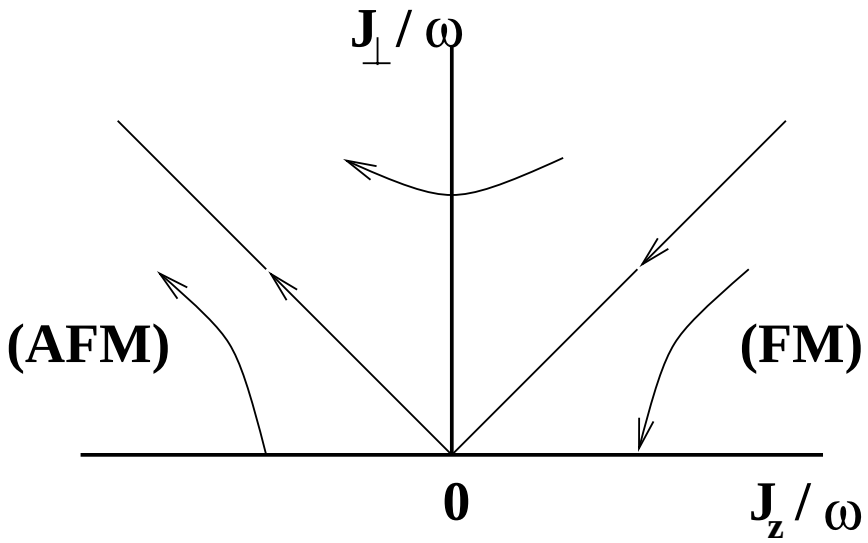

FIGURE 10. Renormalization flux diagram for the Kondo problem near the fixed point of zero coupling.

impurity is frozen, but virtual excursions into it generate local interactions on nearest neighbors. The screening of the impurity spin arises from a shell of width $k_B T_K$ around the Fermi surface.

Within this picture, it is easy to understand the T-dependence of the resistivity, susceptibility and specific heat of metals with magnetic impurities. The scattering events can be thought of as be governed by a temperature dependent cross section. At very low temperatures the impurity is completely screened but the residual interaction between the conduction electrons and the singlet leads to an enhancement in the density of states near the impurity. This is reflected in an increase of the resistivity as the temperature drops below the Kondo temperature while at high temperatures Fermi liquid behavior is recovered. The impurity affects in a similar way the specific heat $\delta C = \gamma(T)T$, with $\gamma = 0$ at high temperatures. The formation of the singlet also quenches the contribution of the impurity spin to the magnetic susceptibility, which approaches a constant at zero temperature. From the low temperature values of the susceptibility and the change in the specific heat it is possible to form a universal constant, the Wilson ratio $(\frac{C}{\chi T})$, in which the only parameter which characterizes the low temperature behavior, the Kondo temperature, drops out.

The Kondo model can be also mapped [7] into the resonant level model. Its Hamiltonian

$$H = \sum_k \epsilon_k c_k^\dagger c_k + t \sum_k (c_k^\dagger d + d^\dagger c_k) + \frac{V}{N} \sum_{k,k'} (c_k^\dagger c_{k'} - \frac{1}{2})(d^\dagger d - \frac{1}{2}) \qquad (127)$$

was introduced to describe a d-level [8] near the Fermi surface interacting with a band of spinless fermions which interact with each other via a repulsive contact

potential (representing the Coulomb interaction). It is important to have in mind that the mapping of these models is valid at low temperatures and for large times where the physics they display is very similar.

Wilson's numerical renormalization group approach

Although the existence of a strong coupling regime in which the impurity is screened forming a singlet was postulated in the 60's this picture was not completely accepted for a long time, because it was not clear that the weak and the strong coupling limits were continuously connected. In the 70's Wilson [3] treated the Kondo problem within a novel numerical renormalization group approach and found the operators which govern the crossover region between the two regimes. An intuitive formulation of field theoretical renormalization group schemes was put forward by Kadanoff, in which he proposed that the running coupling constants used in field theory could be associated to effective Hamiltonians valid for the low energy behavior of blocks of different sizes. This idea was formulated in a more precise way by Wilson. In a quantum system, an effective low energy Hamiltonian is given by the projection of the full Hamiltonian in a restricted basis which contains the low energy states. In such a basis, the intra and interblock couplings can be separated, and the latter treated perturbatively. Wilson's idea was to make this procedure, rooted in the basic approximation schemes of quantum mechanics, iterative. In such a way, it is possible to treat larger and larger blocks, at the cost of reducing the range in energies spanned by the states in the basis. While this method does not converge too well in extended systems, it gives excellent results for impurity problems. This scheme is the starting point of the so called Wilsonkian reformulation of the Renormalization Group techniques. It is best applied to models which are renormalizable in the field theoretical sense, but the method is useful for other models which do not meet this requirement.

For the Kondo model, the implementation of these ideas starts by mapping the problem onto a discrete one-dimensional (radial) model. This greatly facilitates the definition of a transformation which builds effective Hamiltonians for larger systems in terms of the information gained from the eigenvalues and eigenfunctions of Hamiltonians of smaller systems. This procedure works iteratively. For a system of a given size, the Hamiltonian is diagonalized. The low lying eigenvectors are enlarged, by adding the next unit. The Hamiltonian, which now includes the terms which describe the new unit and its interactions to the already solved block, is diagonalized in this basis. The new low lying eigenvectors are kept, and a new unit is added. In this way, the exponential proliferation of states, which is the ban of numerical diagonalizations, is kept in check. The procedure keeps, at all stages, a reasonable description of the low energy eigenstates, which suffice to analyze the dynamics, or the thermodynamic properties at low temperatures.

To perform such a calculation, it was obvious that Bloch states were a non suitable basis, because it was necessary to emphasize those states with the largest

interaction with the impurity, namely, those which where closer to it. However, we must also keep in mind that electron states close to the Fermi surface in momentum space, even this implies that they are delocalized in real space, are also very important. At low temperatures only these electrons are thermally excited and the impurity is going to interact mainly with them. A particular kind of tight binding model is used. The states chosen are closer to the localized Wannier states than to the Bloch states. The first state is approximately a Wannier state localized about the impurity, as localized as possible while still being in the conduction band. The remaining states correspond (roughly) to spherical layers surrounding the impurity. The width of the first layer is denoted $\Lambda^{1/2}$. The shells increase in width. All the wave functions in the basis have an average momentum equal to the Fermi momentum. As n increases the nth state is concentrated closer and closer to the Fermi surface; thus the energy scale for these states decreases being $\sim \Lambda^{-n/2}$ for the nth state. The concrete implementation of the method is as follows: first you solve the impurity coupled to the first Kondo state. Then the terms involving the second Kondo state are added and the equations due to the coupling solved. Then the third state is added, then the fourth, and so forth. This corresponds to include energy scales which decrease successively.

As the energy scale analyzed is reduced at each step, it is not convenient to iterate the method beyond the range of temperatures, or energies, of interest. Thermodynamic properties are based on the partition function, and the levels with energies much larger than KT can be neglected, since its weight is exponentially small. Terms in the Hamiltonian much smaller than the thermal energy, can be also neglected, as they do not change the energy of the levels in a significant way. In order to have a good approximation, and having in mind that if we stop the process at the nth iteration, the energy scales lower than $\Lambda^{-n/2}$ are neglected, so $\beta\Lambda^{-n/2}$ must be much smaller than unity[12].

The numerical calculations show that the iterations for zero and strong coupling ($J = -\infty$) led to fixed points. For antiferromagnetic weak coupling [9] it takes place a crossover from zero to strong coupling as the number of iterations increases. As a result, for very low temperatures or zero temperature, the thermodynamics for weak coupling is very similar to the thermodynamics for strong coupling. In the crossover region, no analytic calculations are possible.

The Kondo model has been solved by analytical techniques [10], confirming the existence of the fixed points described above.

Kondo problem for spin larger than 1/2

We now consider the case in which the spin of the impurity is larger than 1/2 [11]. When only one electronic channel is coupled to the impurity, its spin cannot be fully screened. The effective spin is $S-1/2$ instead S with a degeneracy $2S$ instead

[12)] Remember than in the partition function the statistical weight is given by the Boltzmann factor.

of $2S+1$. This effective spin, which includes one conduction electron, interacts with the remaining electrons. The electron trapped near the impurity has its spin antiparallel to the total spin. Even if it is tightly bound, it can perform virtual hops into the next shell. Thus, electrons with spin parallel to that of the electron trapped near the impurity will be repelled from it. In terms of the effective $S-1/2$ spin and the remaining electrons, we obtain a ferromagnetic interaction. The flow of this problem is trivial, and the low temperature properties can be described in terms of a decoupled $S-1/2$ spin and a conduction band. The arguments can be generalized to the case of n conduction channels, provided that $n < 2S$. When $n = 2S$, full screening is possible, and the impurity spin is quenched, as in the $S = 1/2$ case and one channel.

Multichannel Kondo problem

A much more interesting situation arises when $n > 2S$, the so called multichannel Kondo model, first introduced by Nozières and Blandin [12], has attracted a lot of attention. Here the conduction electrons can have many orbital degrees of freedom, e.g. different d-shell orbitals. The N-channel Kondo model [13] describes a single local moment of spin S, due to a magnetic impurity, antiferromagnetically coupled to N distinguishable types of fermions. These fermions live in N identical conduction bands or channels. The simplest Hamiltonian reads

$$H = \sum_{k\sigma\alpha} \epsilon_k c^\dagger_{k\sigma\alpha} c_{k\sigma\alpha} + J \sum_{k,k',\sigma,\sigma',\alpha} \vec{S} c^\dagger_{k,\sigma,\alpha} \vec{\sigma}_{\sigma\sigma'} c_{k'\sigma'\alpha} \tag{128}$$

where α runs from 1 to N, $J > 0$ and the impurity is in general allowed to have an arbitrary spin s with $\vec{S}^2 = s(s+1)$.

Notice that this Hamiltonian is diagonal in the channel index, namely the channel index is conserved. On the other hand, the coupling is channel isotropic, i.e., J does not depend on α. However, channels are not completely independent because they interact indirectly via the memory of the impurity spin. In an analogous way to the single channel Kondo model, the multichannel Kondo model can be thought as an impurity site at $x = 0$ coupled to a single semiinfinite electronic chain, with a Hamiltonian of the form

$$H = t \sum_{i\alpha} (c^\dagger_{i\alpha} c_{i+1\alpha} + c^\dagger_{i+1\alpha} c_{i\alpha} + J \vec{S} c^\dagger_{0,\alpha} \vec{\sigma} c_{0,\alpha}) \tag{129}$$

Let us start studying this model doing perturbation theory in J, in a similar way to the single channel Kondo model [11]. The flow equations for J

$$\frac{J}{dlnW} = -\rho J^2 + \frac{N}{2} \rho^2 J^3 + O[N J^4] \tag{130}$$

with W a high energy cutoff of the order of the band width and ρ is the density of states. We see that the leading term is unaffected by the number of channels

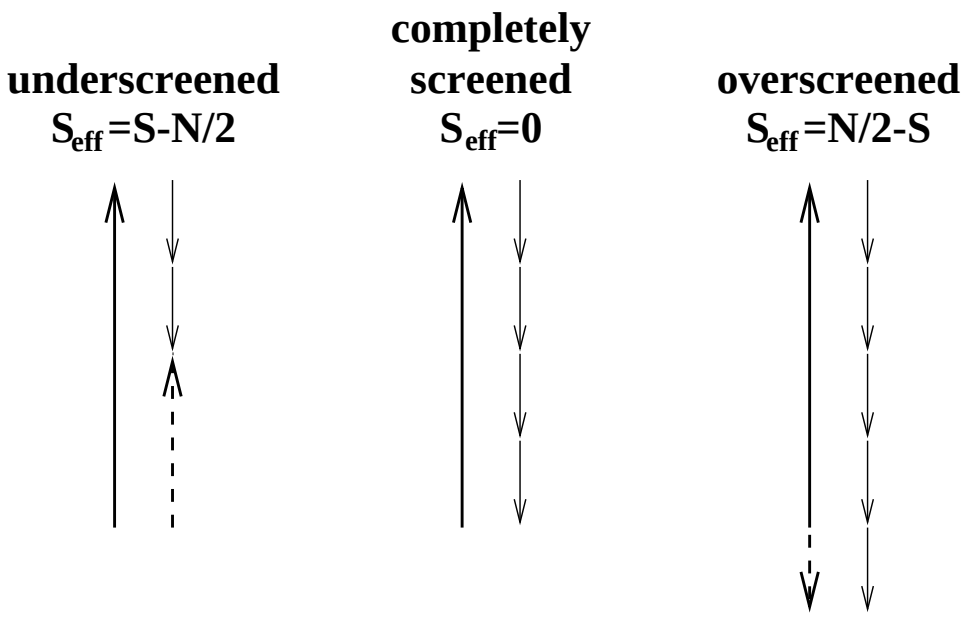

FIGURE 11. Effective residual spins in the strong coupling limit of the multichannel Kondo problem.

and has the same form than for the single channel problem. To leading term, the renormalized coupling constant diverges at a scale T_K given by $T_K \sim W_0 e^{-1/\rho J_0}$, where the subscript zero denotes bare values. However, if N is large, it must include the cubic term. Taking this term into account, we find a fixed point at $J_c = 2/(\rho N)$. This non trivial fixed point implies the existence of critical behavior[13]. Higher order terms are negligible for $N \gg 1$.

Does then our system flow to strong coupling as in single channel case? Let us assume that this is the case and see what happens. In the limit $J/t \longrightarrow \infty$ it is only necessary to consider the single-site model

$$H = \sum_{\alpha} J \vec{S} c^{\dagger}_{0,\alpha} \vec{\sigma} c_{0,\alpha} \tag{131}$$

As $J > 0$, in order to minimize the energy, all the electrons have their spins antiparallel to the impurity. If $N \leq 2S$, we find the situation described at the end of the previous section. When $N > 2S$, the impurity is overscreened and as a consequence a residual spin, parallel to the screening electrons, of size $|S - N/2|$ is formed. The different situations are displayed in Fig. 11 and are analogous to what happens in the simple Kondo problem for $s > 1/2$.

Now we include perturbatively a finite t . To second order, we see that the energy is lowered, by an amount $\delta E \sim t^2/J$, if the electron at site 1 can hop in and out of site 0. In order to satisfy the exclusion principle, it is only possible when their spins

---

[13] The particular value of J_c can be seen to be unstable if we include in our model channel anisotropy.

are antiparallel to the spins of the screening electrons at site 0. The contribution of the hopping term can be analyzed as a residual Kondo interaction with $|J_{eff}| = |\delta E|$. If the impurity is underscreened, we find the ferromagnetic Kondo coupling described earlier. On the other hand, if the impurity were overscreened the residual spin and the hopping electrons would be antiferromagnetically coupled. In this case, we know from the scaling analysis performed earlier that $J_{eff} \sim \frac{t^2}{J} \longrightarrow \infty$, and the strong coupling fixed point is not stable. This implies that a fixed point must exist at intermediate coupling and, as a result, non trivial exponents appear. This fixed point cannot be associated to a phase shift on the electronic wave function, but, as we will see, it is a non Fermi liquid fixed point. It cannot be reached with perturbation theory, except for $N \gg 1$, where we can do an expansion in powers of $1/N$ [14] and stop our flow equations to third order in J.

This non Fermi liquid behavior makes the overscreened multichannel Kondo model specially interesting. Several approaches have been developed in order to study its properties. Some of its features and thermodynamic behavior has been obtained from the exact Bethe ansatz solution. Conformal Field Theories [15] have been also applied. The later approach provides a clear picture of the separation of spin, channel, and charge excitations at non-Fermi liquid fixed points. Starting from the assumption that the system renormalizes to a particular critical point, it can be exactly studied. Another alternative approaches are the bosonization and the perturbation theory of the Yuval-Anderson type. However these two approaches work only for $S = 1/2, N = 2$. This case is specially important. It is the marginal case, but still yields the non-trivial physics, and it has been postulated to describe a variety of related problems (see below).

Among the properties that the overscreened case displays, the zero temperature entropy has attracted a lot of attention. When there is a non screened magnetic impurity in a system, it presents a zero temperature entropy, S_{imp}. This residual entropy is of the form lng where g is the ground state degeneracy [14]. For zero Kondo coupling $S_{imp} = ln[s(s+1)]$, reflecting the groundstate degeneracy of the free spin. For non zero Kondo coupling and exact screening $S_{imp} = 0$ and for the underscreening case $S_{imp} = ln[s'(s'+1)]$, where $s' = s - N/2$. However, in the overscreening case and the thermodynamic limit it has been found that the entropy tends to a universal non-integer number. This surprising result would imply a non-integer degeneracy. It has been recently pointed out [16] that it is a peculiarity of the infinite size approximation which breaks at very low temperatures.

Another quantity to consider is the specific heat coefficient C_{imp} induced by the impurity. In particular, for the very important $\vec{S} = 1/2$ case, if $N = 1$ $C_{imp} \sim T$, what characterizes a Fermi liquid: $N = 2$ is the marginal overcompensated case and $C_{imp} \sim T/T_K ln(T_K/T)$ and for $N > 2$ C_{imp} shows a power law divergence $C_{imp} \sim T^{\alpha}$ with $\alpha = 1 + (2-N)/(2+N)$. This property is a clear evidence of non-Fermi liquid behavior.

The last property we want to discuss is the *scattering behavior*. Again for the

---

[14] In suitable units.

$\vec{s} = 1/2$ case, if $N = 1$, the scattering of an electron off the impurity generates excitations which are well described in terms of ordinary particles. However, for $N = 2$, the quantum number of the outgoing states do not carry the same quantum numbers as the elementary particles used to define the model. The outgoing state can be visualized as a charged screening cloud which is orthogonal to any state with finite number of particle-hole excitations, as we found in the orthogonality catastrophe.

As seen above, the multichannel Kondo model gives an example of genuine non Fermi liquid fixed point. However, it was realized that magnetic impurities do not give rise to an overscreened Kondo systems, because the usual symmetries in a crystal do not allow for $n > 2S$. The two-channel spin Kondo problem , on the other hand, is an useful model in the description of dynamical, non magnetic impurities immersed in a metal [17], which can be described as an effective two level system. It has been applied to amorphous metals, mesoscopic samples or rare earth and actinide compounds. The most convincing measurement of non-magnetic two-channel Kondo [18] behavior has been found in certain zero-bias anomalies in the conductance of a copper nanoconstrictions [19]. In this case, the spin degree of freedom serves as the flavor which characterizes the conduction channels. Another case, which has been widely studied is the quadrupolar Kondo effect in heavy fermion alloys [20–22]. Here, the impurity ground state is a spin zero orbital doublet, acting as a pseudospin 1/2, which interacts with the two spin conduction channels. The level degeneracies of the U ions has been observed by STM techniques [23]. Some of these alloys are also non-conventional superconductors. It has been argued [20,24] that the two-channel Kondo model provides a link to exotic superconductivity and that can account for the marginal Fermi liquid normal state properties of the high T_C materials.

REFERENCES

1. de Haar W.J., de Boer J. and Van der Berg G.J., *Physica*,**1**, 1115 (1933).
2. Ashcroft N.W. and Mermin N.D., *Solid State Physics*, Saunders College Publishing 1976.
3. Wilson K.G., *Rev. Mod. Phys.*,**47**, 773 (1975).
4. Kondo J., *Prog. Theor. Phys.*,**32**, 37 (1964).
5. Yuval G. and Anderson P.W., *Phys. Rev. B*, **1**, 1522 (1970).
6. Abrikosov A.A., *Physics*,**2**, 5 (1965).
7. Guinea F., Hakim V. and Muramatsuk A., *Phys. Rev. B*, **32**, 4410 (1985).
8. Tsvelick A.M. and Wiegmann P.B., *Adv. Phys.*, **32**, 453 (1983).
9. Nozières P. and Low J., *Temp. Phys.*, **17**, 31 (1974).
10. Andrei N., *Phys. Rev. Lett.*, **45**, 379 (1980); Wiegmann P.B., *Sov.Phys.JEPT Lett.*, **31**, 392 (1980).
11. Nozières P., *Proceedings of the Summer School - Dynamic Correlations in Many Fermion Systems*, V.N. de Cerveira, Portugal, 14 to 25 July (1997).
12. Nozières P. and Blandin A., *J. Physique*,**41**, 193 (1980).

13. Coxk D.L. and Zawadowski, *cond-mat* 9704103. Submitted to Advances in Physics.
14. Muramatsu A. and Guinea P., *Phys. Rev. Lett.*, **57**, 2337 (1986).
15. Affleck I. and Ludwig A.W.W.,*Phys. Rev. B*, **48**, 7297 (1993).
16. Rozhkov A.V., *cond-mat* 9711181.
17. Vladar K., Zawadowsky A. and Zimanyi G., **Phys. Rev. B**,**37**, 2001 (1988); Zarand G. and Vladar K. , *cond-mat* 9706091.
18. van Delf J., Ralph D.C., Buhrman R.A., Ludwig A.W.W. and Ambeokar V., *Ann. Phys.*, **263**, 1 (1998).
19. Ralph D.C. and Buhrman R.A., *Phys. Rev. Lett.*, **69**, 2118 (1992).
20. Cox D.L., *Phys. Rev. Lett.*, **59**, 1240 (1987).
21. Seaman C.L., Maple M.B., Lee B.W., Ghamaty S., Torikachvili M.S., Kang J.-S., Liu L.Z., Allen J.W. and Cox D.L., *Phys. Rev. Lett.*, **67**, 2882 (1991).
22. Andraka B. and Tsvelick A.M., *Phys. Rev. Lett.*, **67**, 2886 (1991).
23. J. G. Rodrigo, F. Guinea, S. Vieira and F. G. Aliev, Phys. Rev. B **55**, 14318 (1997).
24. Sire C., Varma C.M., Ruckenstein A.E. and Giamarchi T., *Phys. Rev. Lett.*, **72**, 2478 (1994).

IV MACROSCOPIC QUANTUM EFFECTS

Introduction

Advances in superconducting technology made possible, in the early 80's, the observation of macroscopic variables in regimes where quantum effects were to be expected. The devices used were small Josephson junctions, and the relevant degree of freedom is the superconducting phase across the junction[15] The extrapolation of the laws of quantum mechanics to the world of macroscopic objects poses many interesting questions. In fact, it is well known that quantum mechanics cannot be understood without recursion to a macroscopic world of classical, well defined variables, which can be used as measurement devices. The limitations due to this situation are best shown in Schrödinger's cat paradox [1].

The new study of macroscopic quantum effects required an understanding of the effects of the external environment on the macroscopic degrees of freedom. Usually, macroscopic bodies are described in terms of a few collective degrees of freedom. This procedure implicitly assumes that the remaining degrees of freedom, $\sim 10^{23}$, can be integrated out. This coupling between these excitations and the collective ones can be incorporated into an effective description of the macroscopic variables, by allowing for noise and dissipation. These effects have been thoroughly studied in classical systems. at the quantum level, we expect that dissipative processes induce loss of coherence and suppression of quantum effects, in general.

In the following sections, we outline a general framework for the study of quantum effects in dissipative systems. To do so, we introduce the simplest model Hamiltonian which correctly describes friction and dissipation at the microscopic level, the so called Caldeira Leggett [2,3]. as it will be discussed below, this model has not only the advantage of its simplicity, but it is also very general, and it describes correctly a variety of different physical situations.

Classical limit

We first describe briefly the known aspects of dissipation in macroscopic, *classical* systems.

In the classical limit the dynamics is described by a Langevin equation [4,5] whose main features are a frictional force $\xi(t)$, which is proportional to the velocity, and an additional fluctuating force. This force describes the residual effects from the microscopic degrees of freedom. at the macroscopic level of the present analysis, we can only know statistical averages of its value as function of time:

---

[15] It is widely considered that the superconducting state is itself a macroscopic quantum object. a solid is also a consequence of quantum mechanics, as the atoms are held apart by the Pauli exclusion principle. The observation of quantum effects in the dynamics of the macroscopic phase of a superconductor is akin to the observation of quantum effects in the dynamics of the center of mass of a solid.

$$\langle \xi(t) \rangle = 0 \tag{132}$$

$$\langle \xi(t)\xi(t') \rangle = K_{cl}(t-t') \tag{133}$$

For a white noise source, the frictional force is local in time and stochastic, and the Langevin equation has the Markovian form

$$M\ddot{q}(t) + M\gamma\dot{q}(t) + U'(q) = \xi(t) \tag{134}$$

where the force is δ -correlated according to

$$K_{cl}(t-t') = 2M\gamma K_B T\delta(t-t') \tag{135}$$

being T the temperature of the environment.

As an a example consider a Josephson junction [6,7], i. e. a weak link between two superconductors. The system can be composed by three layers $S_1 - N - S_2$, where $S_{1,2}$ are two superconductors and N can be an insulating film or a normal metal of thickness d. If d is not too large, $d \simeq 20 - 50\mathring{A}$ for an insulating film and $d \simeq 10^3\mathring{A}$ for a normal metal, the Cooper pairs can tunnel between the two superconductors and a supercurrent I_J flows through the junction.

If the region N is only slightly transparent to the pairs, namely, when the current through the junction is small relative to the critical current in the superconductors, the value of I_J is given by

$$I_J = I_c sin(\varphi_1 - \varphi_2) \tag{136}$$

where $\varphi_{1,2}$ are the complex phases of the order parameters in $S_{1,2}$, and I_c, the maximal current which can pass through the junction, depends on the thickness of N and the absolute value of the order parameters in the two superconductors. I_c decreases as d increases. The current I_J is called Josephson current and has been widely observed.

From the previous expression we can see that the dynamical variable that describes a Josephson junction is the phase difference of the order parameters φ of the two superconductors. It is well known that this macroscopic variable cannot be decoupled from the microscopic degrees of freedom, the quasiparticle excitations which act as a heat reservoir and as a source of phase fluctuations. a simple model to describe this coupling, the so-called resistively shunted junction model [8–11], treats the phase as a classical variable, and the barrier as a linear resistor with its associated classical thermal noise. The phase fluctuations are determined by the capacitance of the junction which mainly depends on the size and geometry of the system. The Ohm's law is supposed to be satisfied. as a result the dynamics of the phase is given by

$$C\frac{d^2(\hbar\varphi/2e)}{dt^2} + \frac{1}{R}\frac{d(\hbar\varphi/2e)}{dt} + I_c sin\varphi - I_x = \tilde{I}(t) \tag{137}$$

where we have assumed that the junction is biased by a external current I_x and $\tilde{I}(t)$ is the noise current. Its associated Gaussian current noise is given by Nyquist's formula

$$S_I(\omega) = \frac{1}{2\pi}\int dt e^{i\omega t}\langle\tilde{I}(t)\tilde{I}(0)\rangle_\omega = \frac{K_B T}{\pi R} \tag{138}$$

Notice that this noise, due to thermal fluctuations, vanishes at $T = 0$.

If we identify $\hbar\varphi/2e$ with a coordinate, the capacitance C with a mass, $1/R$ with a damping constant, the previous expression is equivalent to the Langevin equation of motion of a mechanical particle in a potential U, with

$$U(q) = -E_J cosq - I_x\hbar\varphi/2e \tag{139}$$

where the Josephson coupling energy, E_J, is related to the critical current by $E_J = \hbar I_c/2e$.

Caldeira-Leggett approach

At sufficiently low temperatures, the previous analysis is not sufficient, and quantum effects need to be taken into account. Standard quantization of a classical problem starts from a Hamiltonian or Lagrangian formulation of it, which, in this case, cannot be directly derived from the previous equations of motion. Connection between the classical and the quantum description is best achieved through the path integral formulation of quantum mechanics. This procedure allows us also to define effective theories in which some of the initial degrees of freedom have been integrated out.

In the following, we will write down a full quantum description of a macroscopic degree of freedom coupled to a reservoir made up of a very large number of degrees of freedom. Then we will show, by integrating out the variables which describe the reservoir, that the standard dissipative dynamics of the previous section are recovered.

The simplest model for the reservoir is a set of harmonic oscillators, one for each of the true excitations of the system. At the same level of simplicity, we can take the coupling to the collective variables as linear in the oscillators' coordinates [12]. In usual situations, the coupling between the collective variable and an individual excitation in the environment is small[16]. Each of the oscillators defined here is weakly perturbed, even if the effect of all of them on the external variable is large. When the oscillators are mostly in their ground state, with a small probability of being excited, perturbation theory on the coupling is valid. Of more interest here is that the expansion that one obtains in this way is indistinguishable of perturbative expansions of models where the reservoir is made up of more complex excitations. In particular, a clear correspondence between a bath of oscillators and electronic

[16] it must vanish in the limit when the number of excitations, N, goes to infinite.

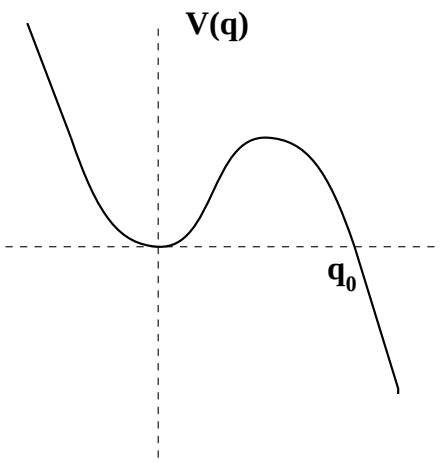

FIGURE 12. We choose an external potential $V(q)$ with a single metastable minimum at $q = 0$

models where the low energy excitations are electron hole pairs, as discussed in previous chapters. Hence, the description of the microscopic degrees of freedom of the system by oscillators is not too restrictive, and a wide variety of problems can be tackled this way.

The model was studied by Caldeira and Leggett [2,3]. As we are interested in the dynamics of the collective variable only, the details of the coupling are not important. Only global constraints, related to its spectral properties, need to be satisfied.

Let us consider a system characterized by some coordinate q in the presence of an external potential $V(q)$ which has a single metastable minimum at a point which we choose as the origin of q. We also choose the origin of energies as $V(0) = 0$. We assume that $V(q)$ is of the form shown in Fig. 12, and in particular $V(q)$ is negative for all points $q > q_0$. We denote q_0 as the exit point, guaranteeing that once the system has left the metastable well, it will have no probability amplitude for returning there in any finite time. This model describes quantum tunneling out of a metastable well. as the particle has no probability of being backscattered into the well, we expect no effects related to quantum coherence between wavepackets. The only non classical process which may arise is the tunneling itself. The classical equation of motion for the system is given by:

$$M\ddot{q} + V'(q) = 0 \tag{140}$$

However, the coupling of the system to the environment introduce dissipation into the behavior of the system, leading to an equation of the type

$$M\ddot{q} + \gamma\dot{q} + V'(q) = 0 \tag{141}$$

If γ does not depend on q we say that the dissipation is linear.

We start from the isolated system and introduce terms in the Lagrangian which couple it to its environment. We have to add two new terms, the "isolated " environment, and the coupling term. The unperturbed Lagrangian of the environmental oscillators is

$$L_{env} = \sum_j (\frac{1}{2} m_j \dot{x}_j^2 - \frac{1}{2} m_j \omega_j^2 x_j^2) \tag{142}$$

and an interaction term which, without loss of generality, may be taken to be of the form

$$L_{int} = -\sum_j (F_j(q) x_j + \frac{F_j^2}{2 m_j \omega_j^2}) \tag{143}$$

The effect of the last term is, simply to ensure that the system cannot lower its potential energy below the original value when the coupling is zero [3]. Thus, the most general Lagrangian which we need to deal with when considering a system weakly coupled (in the above sense) to its environment is

$$L = \frac{1}{2} M \dot{q}^2 - V(q) + \frac{1}{2} \sum_j (\frac{1}{2} m_j \dot{x}_j^2 - \frac{1}{2} m_j \omega_j^2 x_j^2) - \sum_j (F_j(q) x_j + \frac{F_j^2}{2 m_j \omega_j^2}) \tag{144}$$

The classical equation of movement derived from this Lagrangian is, as expected, (141), with γ given by

$$\gamma(q) = \frac{\pi}{2} \sum_j \frac{1}{m_j \omega_j^2} (\frac{\partial F_j}{\partial q})^2 \delta(\omega - \omega_j) \tag{145}$$

If we require the dissipation to be strictly linear $\gamma(q) = cte$, the coupling must be of the form $F_j(q) = q C_j$ and (145)

$$\gamma = \frac{\pi}{2} \sum_j \frac{C_j^2}{m_j \omega_j^2} \delta(\omega - \omega_j) \tag{146}$$

At this point it is convenient to introduce the spectral function of the environmental coupling $J(\omega)$

$$J(\omega) \equiv \frac{\pi}{2} \sum_j \frac{C_j^2}{m_j \omega_j} \delta(\omega - \omega_j) \tag{147}$$

The formalism is very general. For the case of an electrical circuit, such as the resistive Josephson junction, the effect of the dissipation is to add a linear element, whose impedance is

$$J(\omega) = e^2 \omega Re Z(\omega) \tag{148}$$

where $\omega > 0$, since the harmonic oscillators have all positive energy.

In the thermodynamic limit, $J/\omega)$ can be treated as a continuous variable. Then, (146)

$$\gamma = \int_0^\infty d\omega' \frac{J(\omega')}{\omega'} \delta(\omega - \omega') \tag{149}$$

and the expression of the damping coefficient satisfies

$$J(\omega) = \gamma\omega \tag{150}$$

Strict ohmic damping is described by this model with the spectral density of the form (150) for all frequencies ω. This relation describes, of course, an idealized situation. In reality, any realistic spectral density $J(\omega)$ must go to zero when $\omega \to \infty$. Otherwise, certain physical quantities diverge. Clearly, there is always some microscopic memory time scale for inertia effects in the reservoir [4]. The Drude spectral density

$$J(\omega) = \frac{M\gamma\omega}{1 + \frac{\omega^2}{\omega_D^2}} \tag{151}$$

has this fact into account. Here ω_D is a frequency cutoff which defines the memory time $\tau_D = 1/\omega_D$. When the relevant frequencies of a system are much less than the Drude cutoff frequency, the reservoir described by (151) behaves effectively like an Ohmic heat bath.

Another important forms for the spectral density are the cases in which, for low frequencies, it behaves as a power law $J(\omega) \propto \omega^s$. The cases $0 < s < 1$ and $s > 1$ have been popularized as subohmic and superohmic respectively. In the following we are going to restrict us to ohmic dissipation. In this case C_j depends on the frequency on the form:

$$C(\omega) \sim \omega \tag{152}$$

Substituting [17] x_j by $\sqrt{\frac{\hbar}{2m_j\omega_j}}$, the Hamiltonian of our system plus environment model can be rewritten

$$H = \frac{P^2}{2M} + U(q) + \sum_k \omega b_\omega^\dagger b_\omega + \Delta Q \sum_\omega \sqrt{\omega}(b_\omega^\dagger + b_\omega) \tag{153}$$

where Δ is independent of the frequency and the energy of the oscillators and the coupling term have been written in second quantization form. From here we see that the coupling term between the macroscopic variable and the oscillators of the environment for the ohmic case is of the form $\propto \omega^{1/2}$. Notice that this coupling has

---

[17] Remember that a coherent state, namely, an eigenstate of the destruction operator of a harmonic oscillator, satisfies $\langle x_j^2 \rangle = \hbar/(2m_j\omega_j)$ [13]

the same dependence on the oscillators degrees of freedom as the one used in the two-level system problem, where we pointed that this is the type of coupling due to electron-hole excitations. If $U(q)$ is the double well potential, we can restrict our Hilbert space for the macroscopic variable to the two ground states of each minima. This is the case for experiments developed to test Schrödinger's cat paradox [1].

We can use the expression (153) to compare, in a non rigorous way, the energy dissipated per unit time for the classical particle described by (141) and the quantum variable described by (144). Suppose that the potential in (141) has a minimum. Then to a good approximation, near the minimum, the particle moves according to

$$q(t) = q_0 \cos(\omega t) \tag{154}$$

The average energy dissipated per unit time

$$\begin{aligned} \langle \frac{dE}{dt} \rangle &= \gamma \langle \dot{q}^2 \rangle \\ \langle \frac{dE}{dt} \rangle &= \gamma \frac{q_0^2 \omega^2}{2} \end{aligned} \tag{155}$$

Let us now study the quantum particle. If the particle is in the ground state, the average energy dissipated to the environment is given by

$$\langle \frac{dE}{dt} \rangle = \sum_j \langle P_{j0} \rangle E_j \delta(\omega - \omega_j) \tag{156}$$

where j labels the possible quantum states, with energy E_j and P_{j0} is the transition probability between the ground state and j. In second order perturbation theory, P_{j0} can be calculated using Fermi's golden rule. The coupling term can be treated as a collection of sinusoidal perturbations of frequency ω_j. Then the energy dissipated is

$$\langle \frac{dE}{dt} \rangle \propto \gamma \frac{16 \omega^2}{\pi^2} \tag{157}$$

We see that in both cases, classical and quantum particle, the energy dissipated depends in the same way on the frequency.

Finally, it is instructive to note that the environment can be cast as a semiinfinite chain of masses M coupled by springs of restoring force K. This harmonic string is described by a set of equally spaced modes. a coupling of the type considered here, between an additional variable, and all the modes in the environment can be written by means of a term which only involves the mass at the end of the chain and the external variable. as this degree of freedom moves, it radiates sound waves down the chain, which are responsible for the dissipation [14].

Effective action

The Caldeira-Leggett model can be analyzed on a quantum mechanical level [2,3]. as usual, we can determine the equilibrium properties from the canonical density operator $W = Z^{-1}e^{-\beta H}$ where β is the inverse of the temperature, H is the underlying Hamiltonian and Z is a normalization constant. To calculate the density operator is convenient to work in a path integral formalism in imaginary time. To do this, we relate the time-evolution operator $e^{-iHt/\hbar}$ with $e-\beta H$ by means of an analytic continuation, usually called Wick rotation. Doing that we can write the density matrix of our system *particle plus environment* in the form

$$W(q'', x''; q', x') = Z^{-1} \int_{q'}^{q''} Dq(\tau) \int_{x'}^{x''} Dx(\tau) e^{-S^E[q,x]/\hbar} \tag{158}$$

where x is a N-component vector which describes the oscillators' variables and S^E is the Euclidean action, namely the action in imaginary time. This action can be computed from the Euclidean Lagrangian which differs from the original by the reverse sign in the potential term. Our aim is to eliminate the bath degrees of freedom, and to look for an effective action for the macroscopic particle which takes into account the environment effect. If we can do that, the information we are interested in is going to be contained in the reduced density matrix, defined as

$$\rho(q''; q') = \int_{-\infty}^{\infty} dx' W(q'', x'; q', x') \tag{159}$$

$$\rho(q''; q') = \int_{q'}^{q''} Dq(\tau) e^{-S_S^E[q]/\hbar} \int_{-\infty}^{\infty} dx' \int_{x'}^{x''} Dx(\tau) e^{-(S_I^E[q,x] + S_E^E[x])/\hbar} \tag{160}$$

Here S_S^S is the Euclidean action for the particle without taking into account the environment, S_E^E the Euclidean action for the environment and S_I^E the one for the coupling particle-environment. Since the bath is harmonic its degrees of freedom can be integrated out exactly for each possible path of the macroscopic particle. To do that, is useful to write the paths $q(\tau)$ and $x(\tau)$ as Fourier series. This implies that we have chosen these paths as periodically continue outside the range $0 \leq \tau < \hbar\beta$. Then, the integrals in the oscillators variables can be written as gaussian integrals and calculated. We are not going to do it explicitly, but refer the reader to Weiss [4]. Finally we arrive to an expression for $\rho(q''; q')$ in terms only on the particle coordinates

$$\rho(q''; q') = Z^{-1} \int_{q'}^{q''} Dq(\tau) e^{-S_S^E[q]/\hbar} F^E[q] \tag{161}$$

where Z^{-1} is a new constant and F^E can be written as

$$F^E[q] = e^{-S_{diss}^E[q]/\hbar} \tag{162}$$

with $S^E_{diss}[q]$ given by

$$S^E_{diss}[q] = \frac{1}{2}\int_0^{\hbar\beta} d\tau \int_0^{\hbar\beta} d\tau' \alpha(\tau-\tau')[q(\tau)-q(\tau')]^2 \tag{163}$$

The quantity $\alpha(\tau-\tau')$ is defined by

$$\alpha(\tau-\tau') \equiv \sum_n \frac{C_n^2}{4m_n\omega_n} e^{-\omega_n|\tau-\tau'|} \tag{164}$$

$$\alpha(\tau-\tau') \equiv \frac{1}{2\pi}\int_0^{\infty} J(\omega) e^{-\omega|\tau-\tau'|} d\omega \tag{165}$$

From here, we see that for the case of ohmic dissipation, at finite temperature, $\alpha(\tau-\tau')$ is given by the expression

$$\alpha(\tau) = \frac{\gamma}{2\pi}\frac{(\pi/\hbar\beta)^2}{sin^2(\pi\tau/\hbar\beta)} \tag{166}$$

and at $T=0$

$$\alpha(\tau) = \frac{\gamma}{2\pi}\frac{1}{\tau^2} \tag{167}$$

As a result the reduced density matrix can be written in the form

$$\rho(q'';q') = Z^{-1}\int_{q'}^{q''} Dq(\tau) e^{-S^E_{eff}[q]/\hbar} \tag{168}$$

but it involves a non-trivial effective action

$$S^E_{eff}[q] = \int_0^{\hbar\beta} d\tau [\frac{1}{2}m\dot{q}^2 + U(q)] + \frac{1}{2}\int_0^{\hbar\beta} d\tau \int_0^{\hbar\beta} d\tau' \alpha(\tau-\tau')[q(\tau)-q(\tau')]^2 \tag{169}$$

S_{eff} does not contain explicitly the bath degrees of freedom, but it still accounts for the bath and the dissipation through the non-local term.

It is worthwhile to remember that the same effective action has been derived to analyze the motion of a particle coupled to a Fermi liquid [15], where particle-hole pairs are the relevant low-energy excitations, which implies that dissipation is a general feature of fermion environments. It also implies that there are a lot of physical situations in condensed matter which can be described by this phenomenological model. As possible examples, quantum diffusion of particles [16], interstitials [17] inside metals or at the surface [18] or noise and defects in disordered metals [19].

We find another important application of this model in the study of an impurity in a Luttinger liquid [20–23]. In this case, the non local term is associated to the interactions between fermions. The potential, which has a cosine form, to the tunneling through the impurity.

Physical quantities depend on the average $\langle [q(\tau) - q(\tau')]^2 \rangle$, and in particular, we are interested in the behavior for long times or, equivalently, for low temperatures. In the absence of dissipation this function informs us about the time that the wave packet needs to spread. Let us consider first the case in which the potential $U(q)$ vanishes. Then the action is quadratic in the macroscopic coordinate and the integral can be perform. To compute the average we are interested in, we add a term of the form $\lambda(q(\tau) - q(\tau'))$ to the action. Notice that this term is not integrated in imaginary time. It follows

$$\langle [q(\tau) - q(\tau')]^2 \rangle = \frac{1}{Z} \frac{\partial^2 Z}{\partial \lambda^2} \tag{170}$$

The partition function can be written as a path integral over the macroscopic coordinate only.

$$Z = \int dq' \int_{q'}^{q'} Dq(\tau) e^{-S^E_{eff}[q(\tau)]/\hbar} \tag{171}$$

so it is given by

$$Z = \int Dq e^{-\int d\tau \frac{Mq^2}{2}} e^{-\frac{\gamma}{\hbar} \int d\tau d\tau' \frac{[q(\tau)-q(\tau')]^2}{(\tau-\tau')^2}} e^{-\lambda[q(\tau)-q(\tau')]} \tag{172}$$

By means of a Fourier transformation, the partition function can be rewritten as

$$Z = \int Dq e^{-\int d\omega (\frac{M\omega^2}{2} + \omega \frac{|\omega|}{\hbar})(q_\omega + \frac{\lambda}{2} \frac{e^{i\omega\tau} - e^{i\omega\tau'})}{\frac{M\omega^2}{2} + \gamma \frac{|\omega|}{\hbar}})^2} \times e^{-\int d\omega \frac{\lambda^2 |e^{i\omega\tau} - e^{i\omega\tau'}|^2}{4(\frac{M\omega^2}{2} + \gamma \frac{|\omega|}{\hbar})}} \tag{173}$$

Redefining q_ω as

$$q_\omega \longrightarrow q_\omega + \frac{\lambda}{2} \frac{e^{i\omega\tau} - e^{i\omega\tau'}}{\frac{M\omega^2}{2} + \gamma \frac{|\omega|}{\hbar}} \tag{174}$$

it can be seen that the first term in (173) is the partition function of the system Z_S, which can be integrated and does not depend on λ, so that it does not affect the average value we want to calculate. We rewrite the partition function as

$$Z = Z_S e^{-\frac{\lambda^2}{4} \int d\omega \frac{|e^{i\omega\tau} - e^{i\omega\tau'}|^2}{\frac{M\omega^2}{2} + \gamma \frac{|\omega|}{\hbar}}} \tag{175}$$

Finally (170) is given by

$$\langle [q(\tau) - q(\tau')]^2 \rangle = \frac{\partial^2 ln Z}{\partial \lambda^2} = \frac{1}{4} \int d\omega \frac{| e^{i\omega\tau} - e^{i\omega\tau'} |^2}{\frac{M\omega^2}{2} + \frac{\gamma}{\hbar} | \omega |} \tag{176}$$

In the absence of dissipation this is a function which depends on $\tau - \tau'$ on the form $| \tau - \tau' |$, as mentioned before this tells us how the wave packet spreads. In presence

of dissipation, as we are interested in long-time behavior, i.e. $\omega \to 0$, we can neglect the mass term and the dependence is of the type $ln \mid \tau - \tau' \mid$. This implies that the the dissipation leads to a slower rate of the spread of the wavepacket.

Let us introduce now a potential of the form $E_J cosq$ [24]. This is the potential associated to the Josephson junction and as we shall see below, in the renormalization group approach, it is the most general potential which we have to consider for physical situations of interest. If the potential is smooth enough, the contribution to the partition function can be computed from an expansion of the exponential in powers of the coupling constant E_J

$$exp(E_J \int d\tau \cos q(\tau)) = \sum_n \int d\tau_1 ... d\tau_n \frac{E_J^n}{n!} \cos(q(\tau_1)) ... cos(q(\tau_n)) \tag{177}$$

writing the cosines in their exponential form, follows

$$exp(E_J \int d\tau cosq(\tau)) = \sum_n \int d\tau_1 ... d\tau_n \frac{(E_J/2)^n}{n!} \sum_{e_j} e^{i \sum_j e_j q(\tau_j)} \tag{178}$$

where $e_j = \pm 1$. and from this it is straightforward to obtain

$$exp(E_J \int d\tau \cos q(\tau)) = \sum_n \int d\tau_1 ... d\tau_n \frac{(E_J/2)^n}{n!} \sum_{e_j} e^{[i \int d\tau \sum_j e_j \delta(\tau - \tau_j) q(\tau)]} \tag{179}$$

Now, the quantities e_j can be considered as charges of classical particles located at τ_j, but it is important to notice that we have the constraint that the total charge $\sum e_j$ of the particles is zero. That is, we have a neutral gas of charged particles. For $\tau_i - \tau_j \gg \tau_c$, where τ_c is a small times cutoff, the contribution to the action of these particles can be seen to correspond to an interaction between them of the form

$$\frac{1}{\gamma} ln \mid \frac{\tau_i - \tau_j}{\tau_c} \mid \tag{180}$$

In the other limit, $E_J \longrightarrow \infty$, we can use a tight-binding approach. In this case, the particle tends to be localized at one of the minima of the potential, and the tunneling between minima can be well described in the WKB approximation. The tunneling matrix element is thus of the form $t \simeq \sqrt{E_J/M} exp(-C\sqrt{E_J M})$. Then, the path which corresponds to the classical motion of the undamped particle in the inverted potential, instanton [3,11,24,25], gives the dominant contribution to the path integral. These instantons are kinklike solutions. Our variable is expected to be a linear combination of this solutions, which will contribute with different signs. We have taken this into account by constructing a sequence of kinks ($e_j = +1$) and antikinks ($e_j = -1$), which are these classical solutions and again can be thought as electrical charges or Ising variables, located at the positions $\tau_1, ..., \tau_n$, and define the macroscopic variable as

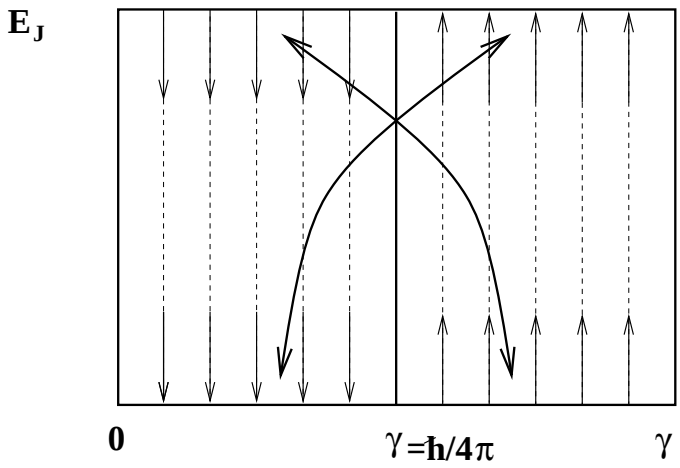

FIGURE 13. RG flow for a Josephson junction. The curved arrows reflect the duality transformation between the perturbative and tight binding limits.

$$q(\tau) = \sum_j e_j f(\tau - \tau_j) \tag{181}$$

On writing the effective action, we can recognize that the charges feel an effective interaction, which at long times behave as $\gamma ln\Lambda \mid \tau_i - \tau_j \mid$, labelling i, j the charges and being Λ a high energy cutoff.

Notice that there exists a duality transformation [24] between the perturbative and tight binding limits

$$t \leftrightarrow E_J \tag{182}$$

$$\gamma \leftrightarrow \frac{1}{\gamma} \tag{183}$$

as is displayed in Fig. 13.

Renormalization group approach

Now, we can obtain a lot of information about the physics of our problem and about the influence of the potential in presence of dissipation, by looking at the parameter space. We will do that within a renormalization group (RG) approach studying the relevant operators [26]. To get familiarize with this technique consider first the action (169) with $U(q) = 0$. This is the free action S_0. a RG transformation consists on integrating high energy modes. If we write our action as an integral in frequencies, this integral goes from 0 to a high frequency cutoff Λ, and the action is denoted as $S_0(\Lambda, 0)$,

$$S_0(\Lambda, 0) = \int_0^\Lambda \frac{d\omega}{2\pi}(m\omega^2 + \frac{4\pi}{\hbar}\gamma \mid \omega \mid) \mid q_\omega \mid^2 \tag{184}$$

then in our RG transformation we integrate over modes for frequencies between Λ/b and Λ where b is a little higher than unity and is usually written as $b = e^{dl} \approx 1+dl$. We split the action in two parts, one for low energy modes and the other for high energy ones, $S_0(\Lambda, 0) = S_0(\Lambda/b, 0) + S_0(\Lambda, \Lambda/b)$. Then we integrate over the strip $\Lambda/b < \omega < \Lambda$. Now, if we can introduce any kind of scale change, in such a way that $S_0(\Lambda/b, 0) = S_0(\Lambda, 0)$, i.e., if we can rescale in a cut-off independent way, we say that our action is scale invariant and that we are at a fixed point. To do that, first, we change $\omega' = \omega b$, so we bring the cut-off Λ/b to the original one Λ. With this change

$$S_0(\Lambda/b, 0) \longrightarrow \int_0^{\Lambda} \frac{d\omega'}{2\pi b}(\frac{m}{b^2}\omega'^2 + \frac{4\pi}{\hbar b}\gamma \mid \omega' \mid) \mid q_{\omega'/b} \mid^2 \tag{185}$$

In order to rescale this action back to original $S_0(\Lambda, 0)$, we can keep m or γ constant upon rescaling. Since we are interested in the properties due to the dissipation we choose γ to be invariant. Then, the mass renormalizes as $m' = m/b$. Taking this into account, we see that q_ω is also renormalized, in the form $q'_{\omega'} = q_{\omega'/b}/b$. Substituting $b \approx 1+dl$ and $m' = m+dm$ we obtain the renormalization group flow equation for the mass

$$\frac{dm}{dl} = -m \tag{186}$$

what implies that the mass decreases as the transformation flows. So we say that the mass is an irrelevant operator. It means that at sufficiently low frequencies the dissipation always dominates over the mass term, and so we can ignore the latter.

Let us look now the effect of the potential. We expand it in a Fourier series

$$U(q) = \frac{1}{2\pi} \sum_{n=-\infty}^{\infty} u_n e^{inq} \tag{187}$$

Here $u_n = u^*_{-n}$ and if the potential barrier has an inversion symmetry, $U(q) = U(-q)$, the u_n are real, so the Fourier series can be rewritten as

$$U(q) = \frac{1}{2\pi}(\sum_{n=1}^{\infty} u_n cos(nq) + \frac{1}{2}u_0) \tag{188}$$

The last term is a constant and we do not need to take it into account, because it can be included in the definition of the energy origin. So we have to analyze how u_n is renormalized under a RG transformation. However, the cosine is a non-linear term and this make the study a little more complicate, but we can calculate it to a good approximation level. Following Castro-Neto [27], we split the macroscopic coordinate into a slow part $q(\tau)^{(-)}$. which contains frequencies in the range from 0 to Λ/b, and a fast part, $q(\tau)^{(+)}$, which contains frequencies in the range $\Lambda/b \leq \omega \leq \Lambda$. In the same way, we split the free action in $S_0^{(-)}$ and

$S_0^{(+)}$, these slow and fast part of the action correspond to previous $S_0(\Lambda/b, 0)$ and $S_0(\Lambda, 0)$. Then we write the partition function as

$$\begin{aligned} Z &= \int Dq^{(-)} \int Dq^{(+)} e^{-S_0^{(-)} - S_0^{(+)} - S_U} \\ &= \int Dq^{(-)} e^{-S_0^{(-)}} \langle e^{-S_U} \rangle_{q^{(+)}} \end{aligned} \tag{189}$$

where S_U is the action associated to the potential. Up to now everything is exact. We assume that u_n is small for all n, then we expand the exponential and re-exponentiate the result

$$\langle e^{-S_U} \rangle_{q^{(+)}} \approx 1 - \langle S_U \rangle_{q^{(+)}} \approx e^{-\langle S_U \rangle_{q^{(+)}}} \tag{190}$$

To calculate this average we have to calculate mean values of operators like $\cos(nq^{(+)})$. Making a redefinition of $q^{(+)}$ similar to (174), it is straightforward to see

$$\langle \cos(nq^{(+)}) \rangle_{q^{(+)}} = e^{-\int_{\Lambda/b}^{\Lambda} d\omega \frac{\hbar}{4\pi} \frac{n^2}{\gamma}} \tag{191}$$

Here we have neglected the mass term, as we have seen that it was an irrelevant operator. Taking into account that $\omega \longrightarrow \omega b$ implies $\tau \longrightarrow \tau/b$, we can obtain the flow equation for u_n

$$\frac{dt}{dl} = (1 - \frac{\hbar}{4\pi} \frac{n^2}{\gamma}) u_n \tag{192}$$

The RG flow is shown in Fig. 13 for a Josephson junction. Notice that for $\gamma > \hbar/(4\pi)$ all the components u_n flow to zero. However, as we decrease γ there is a phase transition and more components become important. For the usual values of γ only the first component is taken into account.

These calculations also predict a transition at $\alpha = \frac{\hbar}{4\pi\gamma} = 1$ between diffusive motion and localization of the macroscopic variable in close analogy to the analysis done for the two level system. In the latter case, in a more rigorous renormalization group treatment a correction to this prediction was necessary. But here there is no such correction because of the translational invariance [28].

Experimental realizations

The models analyzed before describe the quantum effects at low temperatures in Josephson junctions. To be in the quantum regime, the "mass ", that is, the capacitance, should be small enough. In energies, or temperatures, the inequality $e^2/C \ll k_B T, \omega$ must be satisfied (see also the next section). In addition, the states coupled by quantum effects should be macroscopically different.

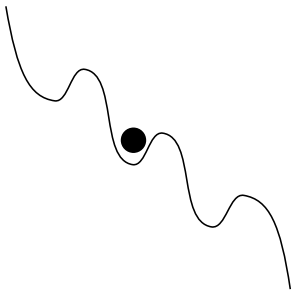

FIGURE 14. Potential for a biased Josephson junction

One of the systems which are suitable to look for macroscopic quantum tunneling is a biased Josephson junction [11]. The potential is given by (139) and its form is shown in Fig. 14. When the phase is localized in one of the minima, the junction is superconducting.

The phase can leave the minimum due to thermal or quantum fluctuations [9,10]. at low temperatures we can neglect thermal fluctuations. Then we have to consider only tunneling processes. The tunneling rate can be calculated for the effective action (169). As was shown by Caldeira and Leggett [2,3] dissipation always tends to suppress quantum fluctuations and, as a consequence, tunneling. As we increase the bias current, the washboard potential is more tilted and is easier for the phase to leave the minimum, when this happens the system is no more superconducting. Each junction has a characteristic critical current [6,7] , which is defined as the maximum current that can support the junction being in the superconducting state. Obviously superconducting and normal states are macroscopically different states. as the dissipation tends to avoid tunneling and to localize the particle, it helps the superconductivity not to be destroyed.

Another of the possible physical systems which satisfies the above conditions is an SQUID [29], namely a superconducting ring interrupted by a Josephson junction. The macroscopic variable is the magnetic flux Φ trapped in the ring. The potential energy of such a system is of the form

$$U(\Phi) = \frac{(\Phi - \Phi_x)^2}{2L} - E_J \cos(2\pi\Phi/\Phi_0) \tag{193}$$

being L the self-inductance of the ring, Φ_x is an applied external flux which pass through the ring and Φ_0 is the flux quantum $\Phi_0 = h/2e$. This potential is displayed in Fig. 15. Again the flux tends to be in a minimum of the potential. If the self inductance is small enough, we can restrict us to the two lowest degenerate minima. We would expect to see resonances between these two states. These states correspond to currents flowing clock-and-anticlockwise around the ring. In particular, tunneling between these two lowest states is usually described by (153) with $U(Q)$ being the two well potential. In the presence of dissipation, these resonances can be destroyed as a result of the localization of the flux in one of the minima.

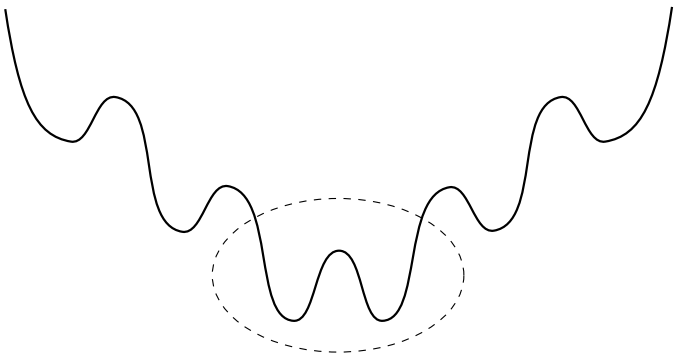

FIGURE 15. Potential in a SQUID. If the self inductance is small enough, only the two lowest minima are important.

Granular materials are systems where dissipation can have also important effects [30] . However, the capacitance of the grains which form these systems is very low and, as we shall discuss in the next chapter, this affects the way in which the coupling has to be analyzed.

At present, here is unambiguous evidence for macroscopic quantum tunneling in Josephson junctions. A striking evidence is obtained by tuning the amount of dissipation by means of an external circuit. The observations are consistent with theoretical predictions to a very high degree.

The case for macroscopic coherence is much less clear. Quantum beats between macroscopically distinct states has not been observed so far. On the other hand, evidence for level quantization in potential wells has been found, in Josephson junctions and in magnetic systems, where the classical variable is the magnetization.

REFERENCES

1. Schrödinger E., *Die Naturwissentschaften*, **23**,807 (1935).
2. Caldeira A.O. and Leggett A.J., *Phys. Rev. Lett.*, **46**, 211 (1981).
3. Caldeira A.O. and Leggett A.J., *Annals of Physics*, **149**, 374-456 (1983).
4. Weiss U., *Quantum Dissipative Systems*, World Scientific, 1993.
5. Van Kampen N.G., *Stochastic Processes in Physics and Chemistry*, North-Holland Personal Library, 1992.
6. de Gennes P.G., *Superconductivity of Metals and Alloys*, New York: W.a. Benjamin, Inc., 1966.
7. Tinkham M., *Introduction to Superconductivity*, McGraw-Hill, 1996.
8. McCumber D.E., *J. Appl. Phys.* **39**, 3113 (1968).
9. Ivanchenko Y.M. and Zilberman L.A., *Zh. Eksp. Teor.Fiz.* **55**, 2393 (1968); *JEPT*,**28**, 1272 (1969).
10. Ambegaokar V. and Halperin B.I., *Phys. Rev. Let.*, **22**, 1364 (1969).
11. Schön G. and Zaikin a.D., *Phys. Rep.*, **198**, 237-412 (1990).
12. Ullersma P., *Physica (Utrech)*, **32, 27,56,74,90**, (1966).

13. Cohen-Tannoudji C., Diu B. and Laloë F., *Quantum Mechanics* Wiley-Interscience, 1977.
14. This very useful representation of the Caldeira-Leggett model was first put forward by A. Schmid, although there is no explicit reference in the literature.
15. Guinea F., *Phys. Rev. Lett.*, **53**, 1268 (1984).
16. Clawson C.W., Crowe K.M., Rosenblum S.S., Kohn S.E., Huang C.Y., Smith J.L. and Brewer J.H., *Phys. Rev. Lett.*, **27**, 2210 (1983).
17. Puska M.J., Nieminen R.M., Manninen M., Chakraborty B., Holloway S. and Nörskov J.K., *Phys. Rev. Lett.*, **51**, 1081 (1983).
18. Schober H.R. and Stoneham A.M., *Phys. Rev. B*, **26**, 1819 (1983).
19. Ludviksson A., Kree R. and Schmid A., *Phys. Rev. Lett.*, **52**, 950 (1984).
20. Kane C.L. and Fisher M.P.A., *Phys. Rev. B*,**46**, 15233 (1992).
21. Guinea F., Gómez-Santos G., Sasseti M. and Ueda M., *Europhys. Lett.*, **30**, 561 (1995).
22. Gómez-Santos G., *Phys. Rev. Lett.*, **76**, 4223 (1996).
23. Schulz H.J., *Fermi liquids and non Fermi liquids*, Proceedings of Les Houches course (1994).
24. Schmid A., *Phys. Rev. Lett.*, **51**, 1506 (1983).
25. Callan C.G. and Coleman S., *Phys. Rev. D*, **16**, 1762 (1977).
26. Shankar R., *Rev. of Mod. Phys.*, **66**, 129 (1994).
27. Castro-Neto A., *Proceedings of the Summer School - Dynamic Correlations in Many Fermion Systems*, V.N. de Cerveira, Portugal (1997).
28. Guinea F., Hakim V. and Muramatsu a., *Phys. Rev. Lett.*, **54**, 263 (1985).
29. *SQUID'85*, eds. Hahlbohm H.D. and Lübbig H., de Gruyter, 1985; Schwartz D.B., Sen B., Archie C.N. and Lukens J.E., *Phys. Rev. Lett.*, **55**, 1547 (1985).
30. Herzog A.V., Xiong P., Sharifi F. and Dynes R.C., *Phys. Rev. Lett.*, **76**, 668 (1996).

V DISSIPATION IN SYSTEMS WITH CHARGING EFFECTS

Introduction

Electron-electron interaction strongly influences electron tunneling in mesoscopic systems. In some cases, it suffices to approximate the Coulomb interaction by an effective capacitance. This is the case in metal junctions where, after a relaxation of the electronic distribution, the remaining Coulomb interaction can be treated as an electrostatic potential, which is well described by the geometric capacitance of the junctions. This capacitance is of the the form $C \sim L\epsilon$, where L is a typical dimension of the island, see Figure 16, and ϵ is the dielectric constant. If our system is built up by two junctions in series, with capacitances C_1 and C_2, the double junction has an effective capacitance $C = C_1C_2/(C_1+C_2)$. It is not obvious why the many body effects that we would expect from the Coulomb interaction among the confined electrons can be taken into account by a constant charging energy. In general, in systems where there are a lot of electrons this approximation, which amounts to the well known Hartree approximation in atomic physics, seems to work well. On the other hand, it fails if the number of electrons involved is small. The transfer by tunneling of one electron between two initially neutral regions, of mutual capacitance C, increases the electrostatic energy of the system by an amount $E_C = e^2/2C$. This energy can be seen as an effective barrier which strongly suppresses the tunneling [1,2].

With the progress in microfabrication technology achieved in the last few years, it has become possible to fabricate in a controlled way metallic tunnel junctions with capacitances in the range of $C = 10^{-15}F$. Similar values can be obtained in quantum dots in 2-dimensional electron gases. Also other systems as granular materials or molecular systems present very small capacitances. Here the capacitance may be as low as $10^{-18}F$.

As mentioned above, the capacitance introduces an energy scale E_C, the charging energy corresponding to a single electron charge, which characterizes all charging effects. It is of order $E_C \simeq 10^{-4}$ eV if the capacitance is $C = 10^{-15}F$, which corresponds to $T = 1K$. Hence we expect transport to be affected by charging effects at $T < 1K$. For capacitances of the order $C = 10^{-18}F$ charging effects are important even at room temperature. Obviously, the highest charging energies which can be attained are comparable to the repulsion between electrons within an atomic level, $\sim$ 1eV, $\sim 10^4$K.

The second energy scale of the system is given by the level spacing, $\delta E \sim (k_F L)^{2-d}\hbar^2\pi^2/m^*L^2$. Here, k_F is the Fermi wave vector, d the dimension, and m^* the effective electron mass. To achieve $\delta E \sim 1K$, one has to reduce the dimensionality or use smaller system sizes. For a $3d$ metallic system with Fermi wave length $\lambda_F \sim 10\mathring{A}$, one needs $L \sim 10nm$. For a $2d$ electron gas it is sufficient to take $L \sim 100nm$. Furthermore, the level spacing is increased in systems with small

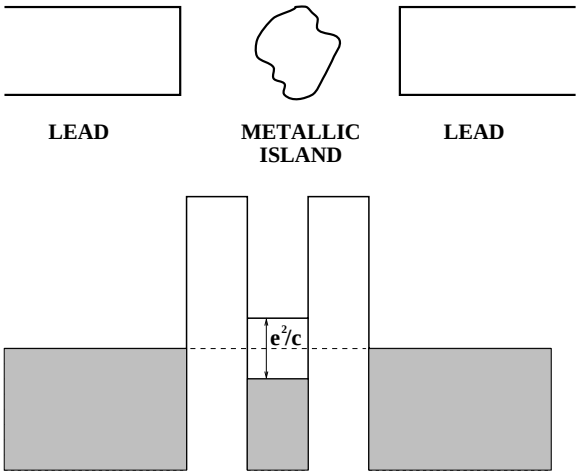

FIGURE 16. The system we consider is a metallic island weakly coupled to two electron reservoirs. In the tunneling process a gap in the density of states of width e^2/C is generated.

effective mass.

We will consider small metallic islands with a large density of states and their generalization to semiconductor quantum dots [3–5]. The basic mechanism [1,2,6,7] at work is the same in both cases, but some important differences arise from the fact that in a metallic island there are a large number of electrons and the level spectrum can be treated as a continuum. In a $2d$ electron gas device there are only a few electronic states, and the level spacing cannot be neglected. It is usual to distinguish between the classical or metallic Coulomb blockade regime, $\delta E \ll K_B T \ll e^2/C$, where many levels are excited by thermal fluctuations, and the quantum Coulomb blockade regime, $K_B T \ll \delta E \ll e^2/C$, which describes semiconductors and where only one or a few levels participate in the transport processes.

Consider the system sketched in Figure 16, where a metallic island is weakly coupled by tunnel barriers to two electron reservoirs. As mentioned above, the island behaves as a capacitor. Suppose that the temperature is low enough so that $(e^2/2C \gg K_B T)$ is satisfied. In the absence of charging effects, one might expect that if we apply a voltage difference between the two reservoirs, electrons could tunnel from one plate of the capacitor onto the metal island and to the other plate of the capacitor. However, because of the Coulomb interaction between electrons residing on the island, the transfer of an electron requires a Coulomb energy $e^2/2C$. Then, for an electron to tunnel onto the island, an energy $e^2/2C$ above the Fermi energy in the contact is required, and a hole needs an energy $e^2/2C$ below the Fermi energy to tunnel. There is a gap in the tunneling density of states of width e^2/C, as shown schematically in Figure 16. The charge in the island changes only by tunneling of electrons to or from the island, and takes integer values. Due to charging effects, the charge is strongly localized in the island for voltages lower than e/C (at $T = 0$), and the conductance is suppressed. The only allowed processes involve the simultaneous transfer at both junctions, and are called cotunneling.

We are interested in junctions which are sufficiently small that charging effects and higher order quantum processes play a role. but large enough so that macroscopic current and voltage sources can be attached to the system and described in a conventional way. Hence, we must include in our description of the quantum dynamics of the junction, plus the external circuit and then study the influence of the electrodynamic environment [8]. We also assume that the transmission per channel at the junctions is much less than unity, so that a standard tunneling Hamiltonian gives a reasonable description. If the system, or part of it, is superconducting new interesting effects can appear [9,10].

Single electron effects

Let us consider a normal junction, characterized by a conductance $1/R_N$. This conductance is related to the usual model Hamiltonians by

$$1/R_N = 4\pi e^2 \mid t^2 \mid N_L(0)N_R(0)/\hbar \tag{194}$$

where $N_{L,R}(0) = mp_F/2\pi^2\hbar^3$ are the densities of states at the Fermi level of the left and right reservoirs and t is the tunneling matrix element. If the junction is driven by an external dc current I_{dc} the charge on the junction electrodes is increased in a continuous fashion, but the charge crosses the tunnel barrier in discrete units of e.

$$\frac{dQ}{dt} = I_{dc} + \frac{\partial Q}{\partial t}|_{tunneling} \tag{195}$$

In a small-capacitance junction the charging energy is the dominant scale and the single-electron tunneling processes act in such a way as to keep this energy small. At low temperatures the transition by single-electron tunneling only occurs if the energy after the tunneling process, which changes Q to $Q \pm e$ is lower than before. This means that the tunneling is blocked as long as the charge on the junction is in the range $-e/2 \leq Q \leq e/2$, but the tunneling is possible if $\mid Q \mid$ exceeds $e/2$. As a result the charge and the voltage across the junction oscillate with a frequency [11–13]

$$f_{SET} = \frac{I_{dc}}{e} \tag{196}$$

This can be understood in an intuitive way. The existence of Coulomb blockade makes that an electron cannot tunnel if the island is in the charged state. On the other hand, the current is the amount of charge which passes through the junction per unit time. So the time which an electron needs to tunnel is $1/I_{dc}$, the frequency of the oscillation is the inverse of this time, and we recover eq. (196). These oscillations are referred as SET (Single-Electron Tunneling) oscillations. The charge oscillations are obviously reflected in the current which passes through the junction. It acquires an ac-component as shown in Figure 17. This property can

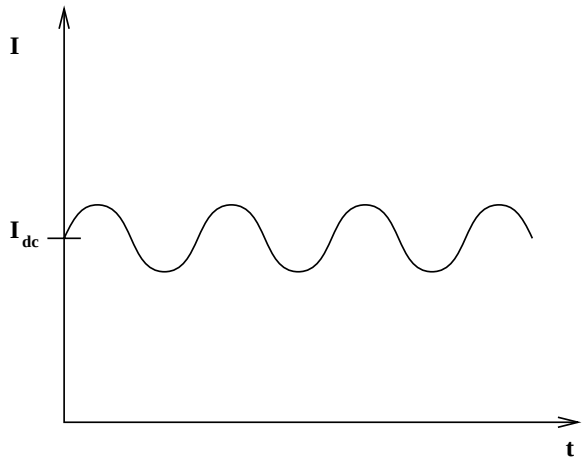

FIGURE 17. The current which passes through the junction presents charge oscillations (Single-Electron Tunneling oscillations). This ac-component can be used for measurement applications.

be used for measurement applications. The reason is that is much easier to get a high resolution in frequency measurements than in current ones. On the other hand, the dc $I-V$ characteristic (for not too small currents) takes the form,

$$\bar{V} \to I_{dc}R_N + (sgnI_{dc})e/2C \tag{197}$$

This picture changes if the temperature increases, because the electrons thermally excited and those involved in cotunneling processes can pass through the barrier. If the temperature is finite but smaller than the charging energy, the dc $I-V$ characteristic is slightly smoothed respect to the $T=0$ case. In the high temperature regime ($K_BT \gg E_C$) , where the discreteness of the charge cannot be discerned, we recover the ohmic behavior. In Figure 18 are displayed the theoretical dc $I-V$ characteristics for different ranges of the temperatures. This behavior can be compared to the experimental curves in Fig. 19.

We now consider a slightly different device. We add the possibility of changing the energy of the island with respect to the reservoirs. This can be done by means of a new terminal, called the gate, which is electrostatically coupled to the island. In this way it is possible to control the particle number on the island. If we turn on a potential difference V_g on the gate, the charge on the island is going to be attracted to the positively charged gate electrode, lowering the energy with respect to the $V_g = 0$ case. Then the electrostatic energy on the island is

$$E = -QV_g + Q^2/2C \tag{198}$$

which up to a constant term can be rewritten as

$$E = \frac{(Q-Q_x)^2}{2C} \tag{199}$$

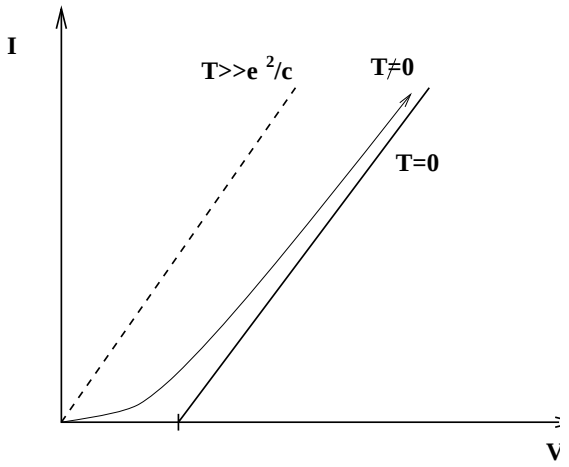

FIGURE 18. Theoretical dc I-V characteristic for different ranges of temperature. The thermal excitations of the electrons are relevant. If the temperature is finite but small the dc I-V characteristic is smoothed and the ohmic behavior is recovered for higher temperatures.

where $Q_x = CV_g$. We can choose any value of Q_x by varying V_g. However, because the charge inside the island is quantized, only discrete values of the energy will be possible for a given Q_x. Now the tunneling processes try to minimize $|Q - Q_x|$, and the current is blocked as in the previous case, except when $Q_x = (N + \frac{1}{2})e$. From (199) we see that when $Q_x = (N+\frac{1}{2})e$, the states with $Q = Ne$ and $Q = (N+1)e$ are degenerate; the charge fluctuates between the two values even at zero temperature, so the energy gap in the tunneling density disappears.

The conductance is thermally activated for all values of the gate voltage except those for which the average charge on the isolated segment is $(N + \frac{1}{2})e$. With increasing gate voltage, the electron number corresponding to the lowest energy state increases [1,13,14]. It does so in discrete steps from N to $N + 1$ at the degeneracy points, see Figure 20. This results at low temperature in a conductance versus V_g curve consisting of periodic sharp peaks. As shown in Figure 20 $\Delta V_g = e/C$. This periodicity can be used to measure the capacitance of the junction. At finite temperatures the steps are washed out and the peaks broadened. In taking into account temperature effects, we have to be careful because the junction can be at a different temperature than the reservoirs [15,16].

There are some important differences in the case that our device is semiconductor, due to the discreteness of the electronic spectrum. At the conductance peaks, the value of Q_x is again equal to $(N + 1/2)e$, but now the Fermi energy in the leads must be equal to that of one of the discrete energy levels of the island. Only if these energies are the same can the charge on the structure fluctuate at zero temperature. This fact influences the amplitude and the position of the peaks. The matching of the Fermi energy with an individual level at a conductance peak requires that the gate voltage difference between two adjacent peaks is e/C plus the energy spacing of the levels of the structure. That is,

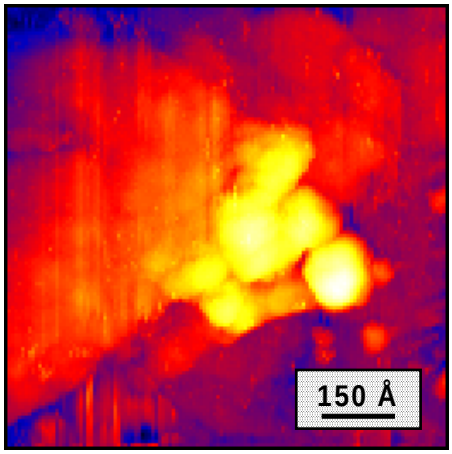

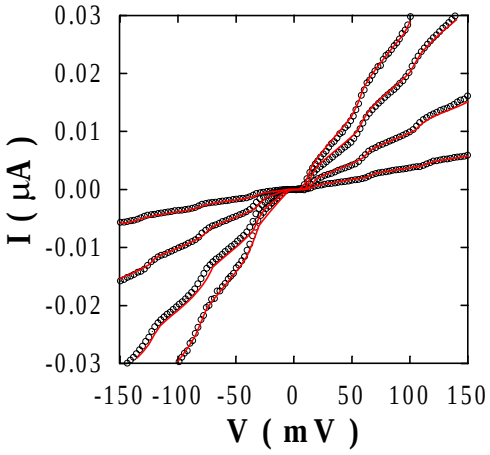

FIGURE 19. The figure on the bottom displays experimental $I-V$ characteristics corresponding to granular superconductors. Its image is shown on the top figure. As the grains are very small, they present Coulomb blockade.

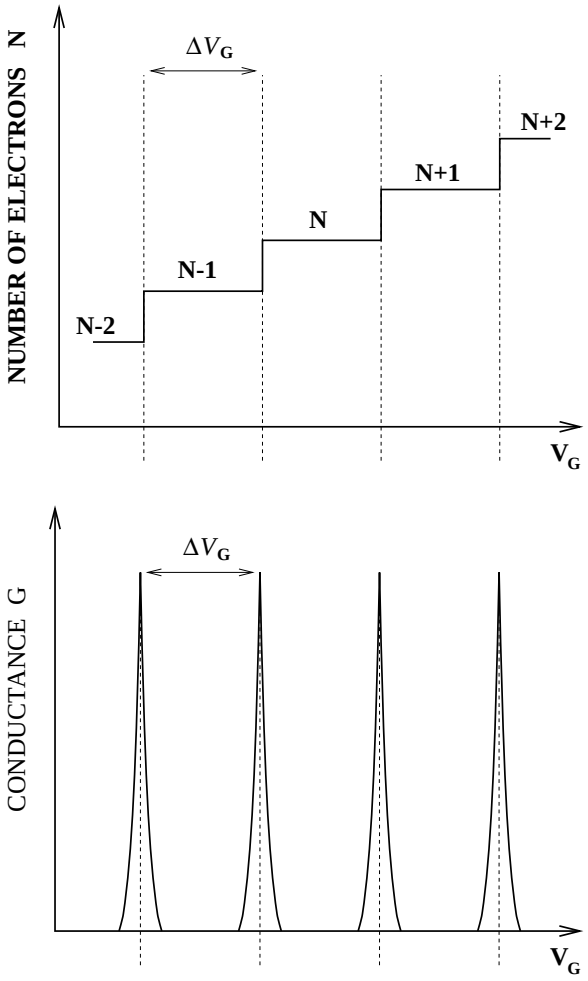

FIGURE 20. When the gate voltage increases, the number of electrons corresponding to the lowest energy state increases in steps. That is why the conductance versus V_g curve presents periodic sharp peaks

$$e\Delta V_N = e^2/C + \delta E_N \tag{200}$$

where ΔV_N is the voltage spacing between the $(N-1)$th and the Nth peaks. This, in turn, means that the peak positions in gate voltage are directly proportional to the energy-level splitting and can be used to measure the level spectrum.

One of the most frequent phenomena associated to charging effects is the so called Coulomb staircase. Consider a double junction, with a metallic island between the two junctions. These junctions have capacitances C_1 and C_2 and tunneling resistances R_1 and R_2. These capacitors carry the charges Q_1 and Q_2 and the metallic island between the junctions carries the quantized charge $Q_1 - Q_2 = Ne$. According to the classical equations the voltage drop in each junction is $V_{1,2} = Q_{1,2}/C_{1,2}$. If the total voltage drop in the double junction is V, the previous expressions can be rewritten:

$$C_1 V_1 - C_2 V_2 = Ne \tag{201}$$

$$V_1 + V_2 = V \tag{202}$$

From these equations the voltages at each junctions are

$$V_1 = \frac{eN}{C_1 + C_2} + V\frac{C_2}{C_1 + C_2} \tag{203}$$

$$V_2 = -\frac{eN}{C_1 + C_2} + V\frac{C_1}{C_1 + C_2} \tag{204}$$

In the case in which $C_1 \ll C_2$, the formulas can be simplified

$$V_1 = V - \frac{Ne}{C_1 + C_2} \tag{205}$$

$$V_2 = \frac{Ne}{C_1 + C_2} \tag{206}$$

We can see that most of the voltage drop takes place at the first junction. If moreover we have $R_1 \ll R_2$, the second junction acts as a bottleneck for the current, which is limited by its value. As shown in Figure 21, the current increases in discrete steps, associated to a change in the average charge in the middle electrode. This curve is known as the Coulomb staircase. At finite temperature these steps are smoothed by cotunneling processes (see below).

In addition, the discreteness of the charge, even in devices which do not show Coulomb blockade effects, gives rise to corrections in the noise spectrum of the current [17].

High order processes: cotunneling

In the theory outlined above we have assumed that the transmission per channel is much less than unity. In this case we can consider that the coupling to the leads

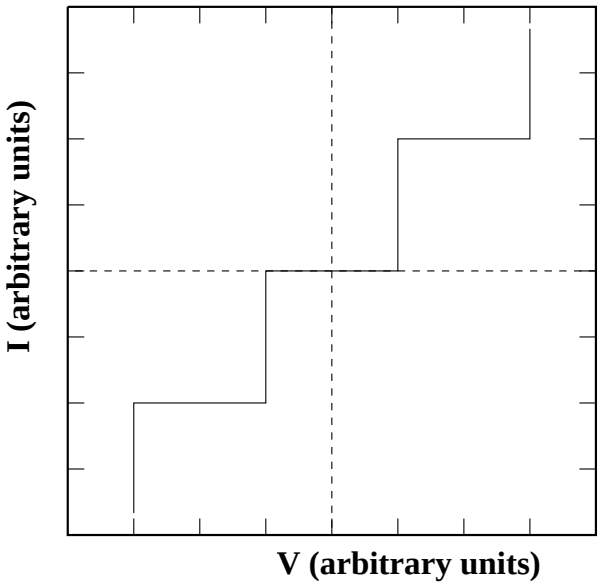

FIGURE 21. If $R_1 << R_2$ the second junction is the one which determines the conductance of the system. It presents a steplike behavior, the Coulomb staircase, reflecting the number of electrons in the island. At finite temperature, these steps are smoothed by cotunneling processes.

does not perturb the levels in the island. If we treat this coupling between the island and the reservoirs by including an intrinsic width $h\Gamma$ of the energy levels, this assumption implies that the broadening of the energy levels is much smaller than the thermal energy even at low temperatures, $h\Gamma \ll K_B T$. First order processes in the tunneling Hamiltonians, as the ones considered in the previous section, are dominant and give rise to sequential tunneling. A proper calculation should not only include direct elastic tunnel events but also tunneling via intermediate states at other energies. Such higher order tunneling processes are referred to as cotunneling events [5,18–20]. These processes are important when sequential single-electron tunneling is suppressed.

As we know, for small bias voltages and low temperatures, $(eV, K_B T \ll 2E_C)$ [18], the sequential tunneling is forbidden , since a single tunneling event would charge the island and increase the electrostatic energy of the system considerably. However tunneling via virtual states is energetically favorable and so allowed. These virtual states have an excess or defect of electronic charge. This tunneling arises due to quantum fluctuations of the charge in the island. As seen before, the charge on the island is a macroscopic variable, and the process can be viewed as a macroscopic quantum process. Because of this tunneling a finite current can flow through the system even in the Coulomb blockade regime.

In second order perturbation theory, the rate of these processes is:

---

[18] If the level spacing δE has to be taken into account the energy scale is $2E_C + \delta E$.

$$\gamma_{i\to f} = \frac{2\pi}{\hbar} \mid \sum_j \frac{\langle i \mid H_T \mid j\rangle\langle j \mid H_T \mid f\rangle}{E_j - E_i} \mid^2 \delta(E_i - E_f) \tag{207}$$

Here E_j is the energy of the virtual state. If we consider a continuous spectrum, the total rate of cotunneling, Γ, is

$$\Gamma \propto (\frac{t^2}{E_C})^2 N_L(0) N_R(0) \tag{208}$$

Here t is the tunneling matrix element between a lead and the island, assumed independent of the state in the lead and island and $N_{L,R}(0)$ are the density of levels at the Fermi energy.

There are two types of processes: inelastic cotunneling, that is, a tunneling process without coherence between tunneling events in the two junctions, and elastic cotunneling, where the same electron tunnels through the total system. These processes are displayed in Figure 22. In an inelastic event, two different electrons tunnel at the two junctions: one jumps into the island above its Fermi level and another one jumps out of the electrode from below the Fermi level. Hence, as a result, an electron-hole excitation is left in the island. In a metallic island, as the energy levels spacing is very small there can be a lot of electron-hole excitations even at low temperatures. Notice that transitions involving different excitations are added incoherently because they label different initial and final states. However for a same initial-final transition there are two channels which add coherently. Either an electron tunnels first from the left lead onto the island, and then an electron tunnels from the island to the other lead, or an electron tunnels first out of the island to the right lead, and another electron from the left lead replaces the charge. These two processes involve different virtual states and their amplitudes have to be added before the matrix element is squared. The current can be calculated according to (207) resulting

$$I(V) = \frac{\hbar}{12\pi^2 e^3 R_L R_R} (\frac{1}{\delta E_L} - \frac{1}{\delta E_R})^2 [(eV)^2 + (2\pi K_B T)^2] V \tag{209}$$

being $R_{L,R}$ the tunneling resistance of the left and right junctions, and $\delta E_{L,R}$ the change in electrostatic energy which suffers the electron when it tunnels through each junction. The inelastic contribution, dominates in the most realistic case when the electron density of states in the island is high enough, as is the case of a metallic junction. The rate of the elastic tunneling depends, in general, on the geometry of the junctions and compared to the inelastic cotunneling rate is smaller by a prefactor which is inversely proportional to the number of states of the island. Only when the tunneling is through a single-level quantum dot or at very low voltages and temperatures it is the dominant process. This is due to the linear dependence of elastic cotunneling in the applied voltage. However, as the temperature increases, the elastic conductance becomes exponentially small, $I_{el} \simeq exp(-K_B T/E_I)$, where E_I is a characteristic energy scale of the island.

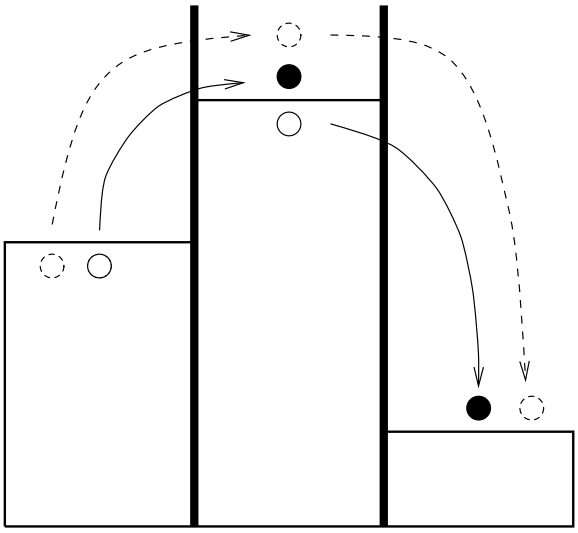

FIGURE 22. Scheme for the cotunneling processes. Solid lines stand for inelastic processes which are much more probable than elastic ones, plotted with dashed lines.

In general, the contribution of these higher processes lead to a significant deviation from "orthodox theory" even in regimes where sequential tunneling contributes. The cotunneling effects can be reduced putting several junctions in series, in devices such as the turnstile [13,21,22] . In systems with N junctions a corresponding N-th process leads to a current $I \propto V^{2N-1}$. However, even in these systems, the cotunneling processes limit the accuracy of the single-electron tunneling.

In addition to higher order tunneling mediated by the Coulomb interaction, the effects of *spin interaction* between the confined electrons and the reservoir electrons can also influence transport properties. When coupled to reservoirs, an island with a net spin, for instance if there is an odd number of electrons, resembles a magnetic impurity coupled to the conduction electrons in a metal. The screening of the localized magnetic moment by the conduction electrons leads to the Kondo effect [5,23] (see chapter devoted to this effect). The energy that determines whether Kondo physics will be visible is $K_B T_K$ where T_K is the Kondo temperature. Below Kondo Temperature, if there is an unpaired electron with a i free spin, it can form a singlet with electrons at the Fermi level in the leads. This coupling results in an enhanced density of states at the Fermi level in the leads and hence an enhanced conductance. The extra electron in the island couples to electrons in both leads, giving an enhanced density of states at both Fermi levels. Raising the temperature destroys the singlet and attenuates the conductance.

In usual SETs, the level splittings are far too small to observe Kondo phenomena. It has been achieved only recently in a semiconductor SET, small enough to permit T_K comparable to accessible temperatures [23].

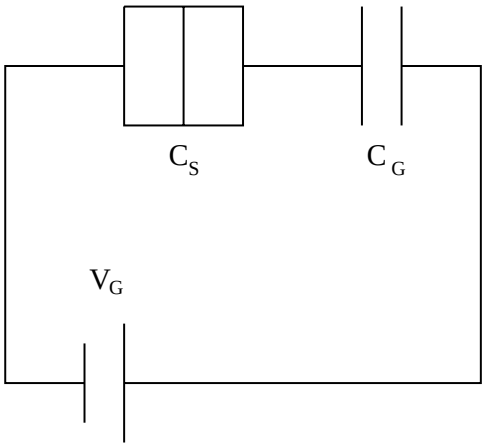

FIGURE 23. Single-electron box.

Single electron devices

As seen before, the charging effects can be used to control single electron charges, which can be applied in different devices. Here we present a brief description of the most simple and important devices [24] which exploit this fact.

The first example is the single-electron box, shown schematically in Figure 23. It consists of a small metallic island, coupled via a tunnel junction with capacitance C_S to an electrode and via a capacitor C_G to a gate voltage source V_G. The charging effects are characterized by (199), with $Q_x = C_G V_G$ and $C = C_G + C_S$. If a gate voltage is applied the number of excess electrons on the island can change due to tunneling across the junction in discrete steps.

Another fundamental example is provided by the single-electron transistor [1,25–29], shown in Figure 24. Here an island is coupled via two tunnel junctions to a transport voltage source $V = V_L - V_R$, such that a current can flow. V is usually called bias voltage. The island is, furthermore, coupled capacitively to a gate voltage V_G. The charging energy of the system is again given by (199), now it depends on the integer number of electrons on the island, as before, and on the three continuous voltages. Q_x is given by $Q_x = C_G V_G + C_L V_L + C_R V_R$, and the total capacitance of the island by $C = C_G + C_L + C_R$, being $C_{L,R}$ the capacitances of the left and right junctions. If we set $V_L = V_R$, we recover the single electron box.

Another devices are the electron trap, similar to the electron box, but with two junctions in series, the electron turnstile [13,21,22], in which two traps are combined and the single-electron pump, where a current is driven by two phase-shifted ac-voltages applied to different islands.

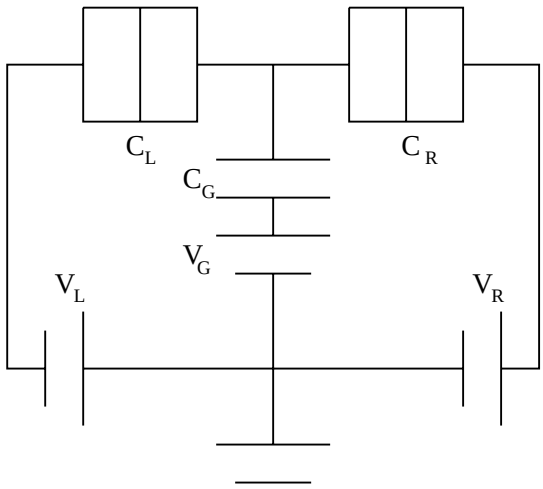

FIGURE 24. Single-electron transistor.

Dissipative Josephson Junction

In the previous chapter we have introduced the classical description of a dissipative Josephson junction. The junction was treated as a classical object which state is characterized by a sharp value of the phase difference across the junction, which is assumed to be shunted by a parallel Ohmic resistor. We have also shown how ohmic dissipation can be obtained coupling the macroscopic variable to the environment, described in terms of harmonic oscillators. This treatment is suitable if the junction has a sufficiently large capacitance and at high temperatures. In this regime, ($E_C << K_B T$), thermal dissipation dominates over tunneling.

On the other hand, for junctions with small capacitance and at low temperatures the classical description is no longer enough. Hence, to take into account charging effects, we have to describe the Josephson junction in a fully quantum mechanical way.

Let us consider first a non dissipative Josephson junction. It can be described by the Hamiltonian

$$H_0 = \frac{Q^2}{2C} + U(\varphi) \tag{210}$$

This Hamiltonian gives the eq (137) in the classical limit. In an unbiased Josephson junction we can realize a perfectly periodic potential, due only to the Josephson coupling, see (139).

Notice that as the charge on the junction and the phase difference are conjugate variables, whose commutation relation is $[Q, \hbar\varphi/2e] = \hbar/i$, this problem is equivalent to the particle in a periodic potential. We can consider the potential as a 2π periodic extended potential and interpret the eigenstates as Bloch states [30–33] labelled by a pseudo momentum Q_x, i.e. $\psi_{n,Q_x}(\varphi + 2\pi) = \exp(i2\pi Q_x/2e)\psi_{n,Q_x}(\varphi)$.

Alternatively, we choose a gauge where the wave function is 2π-periodic and the charging energy in H_0 is replaced by $(Q+Q_x)^2/2C$. Then the new Hamiltonian is

$$H_0^{Q_x} = (Q+Q_x)^2/2C - E_J cos\varphi \tag{211}$$

The classical gauge field Q_x can be interpreted as an external charge on the junction electrodes, created by the flow of a weak current through the leads. But on taking into account the dissipation, there exists an important difference between the external charge Q_x on the junction electrodes and the actual charge. The former is fixed by external constraints,which may be so strong that we can ignore fluctuations in Q_x and treat it as a classical variable. The second fluctuates due to the possibility of tunneling across the barrier. Because of Cooper pair tunneling, the actual charge on the electrodes can take the values $Q = Q_x + n \cdot 2e$ with n integer. The energy levels thus form $2e$-periodic energy bands. The detailed form of $E_n(Q_x)$ depends on the ratio between the charging energy scale and the Josephson coupling energy. They are displayed in Fig. 25 for the limits $E_C \ll E_J$ and $E_J \ll E_C$. In order to make connection with a normal tunnel junction, we can define a collective variable conjugate to the total charge, with the associated commutation relation $[Q, \hbar\varphi/e] = \hbar/i$ and then it is only necessary to impose $E_J = 0$. Notice that the commutation relation for the metallic and superconducting junctions are the same with a different choice for the elementary charge, reflecting the fact that in a normal junction there are no Cooper pairs but only fermions. In both cases we can find a relation between the phase and the voltage which drops in the junction. As usual the current which pass through the junction is defined as $I = \dot{Q}$ and the potential drop is written as $V = Q/C$. Then, exploiting the fact that Q and the phase φ are conjugate variables

$$\frac{d(\hbar\varphi/e^*)}{dt} = \frac{Q}{C} \tag{212}$$

where e^* is the elementary charge associated to each junction. The phase and the voltage through the junction are related by

$$\dot{\varphi} = \frac{e^*}{\hbar} V(t) \tag{213}$$

We want now to introduce dissipation in our Josephson junction. It is produced by the quasiparticle tunneling, so we have to worry about charging effects when the capacitance of the system is small. Besides, the junction must reflect the periodic behavior that we have found in the previous case where dissipation was neglected. Now , because of the transitions caused by quasiparticle tunneling [30–33] , the energy bands are e-periodic in Q_x and their number is doubled.

If we introduce dissipation in the way that Caldeira-Leggett do it [34], the effective Hamiltonian of the system is

$$H = \frac{Q^2}{2C} + E_J cos2\varphi + \alpha_0 \int_0^{\tau_c}\int_0^{\tau_c} d\tau d\tau' \frac{(\varphi(\tau)-\varphi(\tau'))^2}{(\tau-\tau')^2} \tag{214}$$

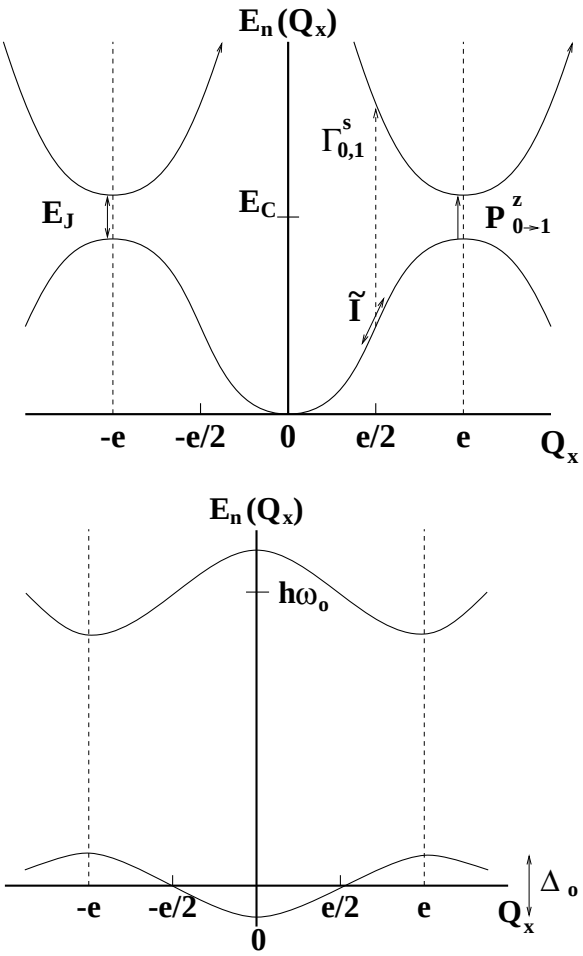

FIGURE 25. Energy bands associated to a non dissipative Josephson junction. The top figure displays the case $E_C \ll E_J$, while the bottom figure shows the $E_J \ll E_C$ limit.

with α_0 given by

$$\alpha_0 = \frac{\hbar}{2\pi e^2 R_N} \tag{215}$$

It is no more gauge invariant, but it changes the charge in arbitrary units. This approach, as we have previously seen, describes ohmic behavior, but it is no longer valid when quantized charge processes take place. Then, the theory of the quantum mechanics of the phase variable has to be constructed from a microscopic model of superconducting tunneling [33,35].

Let us start from the Hamiltonian

$$H = H_L + H_R + H_T + H_Q \tag{216}$$

where $H_{L,R}$ describe the superconductors on the left and right of the junction, H_T is the tunneling Hamiltonian and H_Q is the Coulomb energy associated with charge transfer across the junction. Explicitly we take

$$H_{L(R)} = \int d^3x \psi^\dagger_{L(R)\sigma}(x)[-\frac{\hbar^2}{2m}\nabla^2 - \mu]\psi_{L(R)\sigma}(x)$$
$$- \frac{g_{L(R)}}{2}\int d^3x \psi^\dagger_{L(R)\sigma}(x)\psi^\dagger_{L(R)-\sigma}(x)\psi_{L(R)-\sigma}(x)\psi_{L(R)\sigma}(x) \tag{217}$$
$$\tag{218}$$

$$H_T = \int_{x\in L} d^3x \int_{x'\in R} d^3x'[T_{xx'}\psi^\dagger_{L\sigma}(x)\psi_{R\sigma}(x') + H.c.] \tag{219}$$

$$H_Q = \frac{1}{2C}(\frac{Q_L - Q_R}{2})^2 \tag{220}$$

Here $\psi_{L(R)\sigma}$ is the electron field operator in the left (right) side with spin σ and repeated spin indices are summed over. The range of the tunneling matrix element $T_{xx'}$ is restricted to the vicinity of the oxide barrier, and the charge on the left and right side are defined as

$$Q_{L(R)} = e\int d^3x \psi^\dagger_{L(R)\sigma}(x)\psi_{L(R)\sigma}(x) \tag{221}$$

As before, it is convenient to work in a path integral description derived from the Hamiltonian. Restricting our attention to the phase difference across the junction, the following action can be derived [33,35]:

$$S = \int_0^{\hbar\beta} d\tau[\frac{C}{2}(\frac{\hbar\varphi}{2e})^2 - E_J\cos\varphi] + \hbar\int_0^{\hbar\beta} d\tau \int_0^{\hbar\beta} d\tau' \alpha(\tau-\tau')\times[1-\cos\frac{\varphi(\tau)-\varphi(\tau')}{2}] \tag{222}$$

The first term contains the charging energy and the Josephson coupling. The second term accounts for the quasiparticle tunneling. The term which describes dissipation in the present case has a non linear dependence on the phase, instead of the quadratic term used in the Caldeira-Leggett description. This dependence arises from the discreteness of the elementary charge transfer process. The explicit expression of the kernel $\alpha_{qp}(\tau)$ depends on the detailed properties of the system, and reflects the features of the quasiparticle current-voltage characteristic $I_{qp}(V)$. Both quantities are related by [32,33]:

$$\alpha(\omega_\nu) = \frac{\hbar}{e} \int \frac{d\omega}{2\pi} \frac{\omega}{\omega^2 + \omega_\nu^2} I_{qp}\left(\frac{\hbar\omega}{e}\right) \tag{223}$$

We can estimate the shape of α_{qp} in certain limiting cases:

(a) In an ideal junction with a perfect BCS density of states, i.e., if there exists no pair-breaking effects, the quasipartice current vanishes for $\mid V \mid < 2\Delta/e$. In this case $\alpha_{qp}(\omega_\nu)$

$$\alpha_s(\omega_\nu) = \begin{cases} -\frac{3\pi^2 \alpha_0 \hbar \omega_\nu^2}{32\Delta} & \text{if } \mid \hbar\omega_\nu \mid \ll \Delta \\ -\alpha_0 \pi \mid \omega_\nu \mid & \text{if } \mid \hbar\omega_\nu \mid \gg \Delta \end{cases} \tag{224}$$

or in terms of the imaginary time

$$\alpha_s(\tau) = \hbar\alpha_0 \begin{cases} 1/\tau^2 & \text{for } \mid \tau \mid \ll \hbar/\Delta \\ \frac{\pi}{2}(\frac{\Delta}{\hbar})^2 \frac{\hbar}{\Delta\mid\tau\mid} \exp(-\frac{2\Delta\mid\tau\mid}{\hbar}) & \text{for } \mid \tau \mid \gg \hbar/\Delta \end{cases} \tag{225}$$

We have assumed that the order parameter in the two superconductors is the same. In some problems we need to consider only small frequencies and small variations of the phase difference, that is, the phase varies only slowly in time on the scale given by $\hbar/\Delta$. In these cases we can expand the trigonometric function in the dissipative term which leads to [35]

$$S_\alpha \simeq \frac{\hbar}{4} \int d\tau (\partial\varphi/\partial\tau)^2 \int d\tau' \alpha(\tau') \tau'^2 \tag{226}$$

In this form we see that the effect of the tunneling of quasiparticles under the given conditions is the renormalization of the capacitance by

$$\delta C = 3\pi\hbar/32\Delta R_N \tag{227}$$

(b) In a normal junction, that is, for $\Delta = 0$ the kernel $\alpha(\tau)$ coincides with the kernel found for Ohmic dissipation [34]

$$\alpha_t(\tau) = \alpha_0 \frac{(\pi/\hbar\beta)^2}{sin^2(\pi\tau/\hbar\beta)} \tag{228}$$

$$\alpha_t(\omega_\nu) = \pi\alpha_0 \mid \omega_\nu \mid \tag{229}$$

Note that, even with the same kernel, we have not recovered the Ohmic contribution because the action still depends on the phase difference in a trigonometric fashion.

(c) On the other hand, if the density of states have a non-perfect energy gap because of paramagnetic impurities or because of a suppression of superconductivity in part of the junction, even at $T = 0$, the junction has a finite subgap conductance $1/R_{qp}$. In this case $\alpha_{qp}(\omega)$ acquires a contribution of the form (228). It is an experimental observation that the subgap conductance in very small junctions is not negligible. Then we can approximately account for this subgap conductance by using $\alpha(\tau) = \alpha_s(\tau)+\alpha_t(\tau)$ where α_s is given by (225) and α_t by (228) with $R = R_{qp}$ in the expression of α_0. We take R_{qp} as an input parameter from the experiment. Then the effective action of the system is of the form (222) where the capacitance contains the correction (227) and $\alpha(\tau)$ depends on the subgap conductance $1/R_{qp}$. Note that if we set $\Delta = 0$ and replace it in the α terms and the trigonometric functions by their small argument expansion this description reduces to the one derived by Caldeira and Leggett [34]. Conversely, the phase-related features of our model can be obtained by a generalization of Caldeira-Leggett's model, coupling the macroscopic variable to two independent ensembles of harmonic oscillators. That is easy to see. Starting from H_0 given by (210) and from the commutation relations between the charge and the phase, the coupling to the electrodes and the dissipation due to it can be described by the Hamiltonian [32,33]

$$H = H_0 + \sum_{\alpha=L,R} \sum_k \varepsilon_k c^\dagger_{k,\alpha} c_{k,\alpha} + \frac{1}{2N(0)} (\frac{\alpha}{2})^{1/2} e^{i\varphi/2} \sum_{k,k'} c^\dagger_{k,L} c_{k',R} + h.c. \qquad (230)$$

The second term describes the energy of the electronic band of both reservoirs, while the last one describes tunneling between the left and right electrodes. The factor $e^{i\varphi/2}$ ensures that the charge changes by unity (e and not $e^* = 2e$) when a tunneling event occurs. In close analogy to the bosonization procedure developed in the chapter devoted to the orthogonality catastrophe, (230) can be rewritten as

$$H = H_0 + \sum_{p>0} v_F p(b^\dagger_p b_p + b'^\dagger_p b'_p) + (\frac{\alpha}{2N(0)})^{1/2} \sum_{p>0} [cos\frac{\varphi}{2}(b^\dagger_p + b_p) + sin\frac{\varphi}{2}(b'^\dagger_p + b'_p)] \qquad (231)$$

Notice that two independent oscillator baths have been necessary. If we derive an effective action integrating out the oscillators as done in previous chapter, we cannot obtain a nonlocal trigonometric interaction term with only one bosonic bath. The other important difference between this bosonic Hamiltonian and the one used in the previous chapter to derive Caldeira-Leggett's action, is that the functions which couple the macroscopic variable, i.e. the phase, to the bath, are nonlinear.

Critical behavior

We want to study the critical behavior of (222) where the effect of the gap is assumed to be included in the capacitance and α is given by (228). Due to the

trigonometric term, this action cannot be directly mapped onto an Ising model but corresponds to the one-dimensional XY model with long range interactions [32,33]. Rigorously, if the expression of α is of the form $\sim \omega^2$ the interaction would be of short range, decaying exponentially, while for α given by (229) the interaction is long range, decaying proportional to $1/(\tau - \tau')^2$ (at $T = 0$) [19]. We can rewrite the partition function and the effective action as [36]

$$Z = \int Dn\delta(n^2 - 1)exp - S[n] \tag{232}$$

$$S[n] = \int d\tau d\tau' \alpha(\tau - \tau')[1 - n(\tau) \cdot n(\tau')] \tag{233}$$

where $n(\tau) = (cos\phi(\tau), sin\phi(\tau))$ may be used to relate the XY spin orientation to voltage using $\dot{\phi}(\tau) = eV/2\hbar$. It is natural to introduce $\phi = \varphi/2$ as a new variable.

The XY model in which our system can be mapped onto, presents an easy axis. While the dissipation term is 2π-periodic in ϕ (4π periodic in φ), the Josephson coupling is 2π periodic in φ, favoring $\phi = 0$ and $\phi = \pi$ equally. This provides an easy axis in the XY plane. E_J gives the strength of this easy axis.

Let us first consider the tight binding limit [32,33] $E_J \gg E_C$. The system tends to be localized in one of the minima of the Josephson potential, and thus the dominant paths of the phase $\varphi(\tau)$ are tunneling events between these minima. The kinks technique is suitable to study this problem. Our instantons are kinks between the different values 0, $\pm 2\pi$, $\pm 4\pi$,..., at times τ_j. Since the dissipation due to tunneling is 4π periodic, it distinguishes only between instantons changing $\varphi(\tau)$ from an even to an odd multiple of 2π or viceversa.

Let us now consider, the Hamiltonian (230) in the tight binding limit. We can restrict our attention to the lowest energy state within each well. This approximation introduces a cutoff of the order of the level spacing in a single potential well [20] $\omega_0 = (8E_J E_C)^{1/2}$. These low energy states are weakly hybridized as a consequence of the tunneling events between the wells. To express it, we introduce a small hopping term, which numerical value would be of the order of the bandwidth in the Bloch description of the junction. It depends on the values of E_J and E_C on the form

$$t = 8(\frac{E_J E_C}{\pi})^{1/2}(\frac{E_J}{2E_C})^{1/4} exp[-(8\frac{E_J}{E_C})^{1/2}] \tag{234}$$

---

[19] The XY model consists of "magnetic compasses" attached to lattice sites, with nearest neighbor interactions. The interaction matrix is of the Ising type. But now our spins do not need to take value $= 1$ or -1 as in the Ising model, the only constraint is to have modulus unity. They can be thought of as complex numbers. The lattice can be (for a general XY model) in any number of spatial dimensions (one-dimension in our case), but the compasses all rotate in the same two-dimensional plane (hence the name XY). The complex phase is the equivalent to the rotation angle.

[20] To obtain the value of the level spacing it is only necessary to expand the cosine term in the Josephson potential and to compare (210) with the Hamiltonian of a one-dimensional harmonic potential.

As in these minima φ is close to $2\pi n$ in the interaction part, $cos(\varphi/2)$ and $sin(\varphi/2)$ can be replaced by $(-1)^n$ and 0 respectively. The Hamiltonian can be rewritten as

$$H = t\sum_n d_n^\dagger d_{n+1} + h.c. + \sum_{p>0} v_F p b_p^\dagger b_p + (\frac{\alpha}{2N(0)})^{1/2} \sum_n (-1)^n d_n^\dagger d_n \sum_{p>0} (v_F p)^{1/2}(b_p^\dagger + b_p) \tag{235}$$

The dissipation term distinguishes only states in odd or even minima. Thus, it is convenient to work in the basis of extended states

$$d_q = \sum_n d_{2n} e^{iqn} \tag{236}$$

$$d'_q = \sum_n d_{2n+1} e^{iq(n+1/2)} \tag{237}$$

such that the hopping connects only a state created by $d_q^\dagger$ with one created by $d_q'^\dagger$. For each q we obtain an effective two-level system

$$H_q = tcos\frac{q}{2}\sigma_x + \sum_{p>0} v_F p b_p^\dagger b_p + (\frac{\alpha}{2N(0)})^{1/2}\sigma_z \sum_{p>0} (v_F p)^{1/2}(b_p^\dagger + b_p) \tag{238}$$

The Pauli matrices are defined in the space spanned by d_q and d'_q. The ground state belongs to the subspace with $q = 0$. From the two-level system analysis [32,33,37–40], we know that our system has a phase transition at

$$\alpha_c = 1 + 2\frac{t}{\omega_c} \tag{239}$$

This transition displays some differences with respect to the one associated to the ohmic Josephson junction, although both are of the Berezinski-Kosterlitz-Thouless type. In the ohmic case the transition occurs at a critical value of α which is independent of E_J. Besides, in the ohmic case above the critical strength of the dissipation the phase is localized in one of the minima of the potential. On the other hand, in our case, above the transition, the phase is localized in the even or in the odd numbered minima.

In the limit of weak Josephson coupling, $E_J \ll E_C$, we can perform a perturbative renormalization group expansion of the Kosterlitz type [32,33,37], but now in powers of $1/\alpha$ around the ordered state. Upon reducing the high-energy cutoff, we obtain the following scaling equations.

$$\frac{d\alpha}{d(ln\omega_c)} = -\frac{2}{\pi^2} \tag{240}$$

$$\frac{d(\frac{E_J}{\omega_c})}{d(ln\omega_c)} = -\frac{E_J}{\omega_c} \tag{241}$$

From the first equation, we see that α decreases in the scaling process, and that the theory is asymptotically free, in an analogous way to Quantum Chromodynamics. Let us restrict to the $E_J = 0$ case, i.e. to a metallic tunnel junction. We expand the effective action (222) up to fourth order in $\varphi(\tau)$ around the Caldeira Leggett limit. The resulting action is again of the Caldeira-Leggett's type

$$S = \int d\omega (\frac{\omega^2}{2E_C} + \tilde{\alpha} \mid \omega \mid) \tag{242}$$

where $\tilde{\alpha}$ has been renormalize by the term to fourth order. The dissipative term will be the most important at low energies where its value is higher than the one due to charging energy. So the charging energy acts as a cutoff. As α decreases with the cutoff, at low scale the Coulomb Blockade effects dominate over the dissipation. Remember that dissipation is due to quantum coherence. Thus, at sufficiently low energy, coherence is lost and transport has to be explained in terms of a granular model [41].

Shake-up effects

Until now we have analyzed tunneling processes within the framework of orthodox Coulomb blockade theory. We have assumed that the charge transfer has a high energy cost, but it does not induce excitations in the electronic system. When the junction jumps from one charge state to another, all energy levels are shifted rigidly, and the electron which tunnels finds itself in an unperturbed electronic state. So if the tunnel junction is initially in thermal equilibrium, the state immediately after tunneling is in another thermal equilibrium. The transient behavior between the equilibrium states before and after tunneling is neglected. This assumption is justified if the potential created by the additional charge (an electron in one electrode and a hole in the other) is very uniform over length scales comparable to the wavelength of the electrons. In small metallic islands, however, the charge is confined to regions bound by the dimension of the device, and the approximation of an homogeneous potential is no longer valid.

In normal tunnel junctions, the electrical relaxation can be separated into two stages, having different time scales. In the first stage, the tunneling electron is screened through the excitation of surface and bulk plasmons, forming the screened Coulomb potential. Following this stage, the electrons at the Fermi level have to rearrange themselves in a new configuration. As they have a much longer response time, they feel the screened Coulomb potential as a sudden and local perturbation. Thus, the perturbation causes a many-body final state in which infinite low-energy electron-hole pairs are excited [42]. This process is analogous to the X-ray singularity problem [43,44], that we have previously studied, where the local perturbation is induced by the sudden removal of a core electron by an X-ray photon. Due to the orthogonality catastrophe [45] , the groundstate of the junction when electrodes are charged is orthogonal to the groundstate of the neutral junction. Thus the charge

transfer may leave the system in a highly excited state. Many body effects not only occur in each electrode separately, but, due to excitonic effects, the tunneled electron is attracted to the positively charged electrode, while the remaining hole is attracted to the negatively charged one. In general, these many-body mechanisms are called shake-up effects.

To examine these effects we consider the microscopic Hamiltonian [46,47]

$$H = H_L + H_R + H_T + H_C \tag{243}$$

where H_T and H_C are respectively the usual tunneling and charging terms, while the Hamiltonian of the electrodes $H_{L,R}$ include the local perturbations. They are of the form [48]

$$H_\alpha = \sum_\alpha \epsilon_{k,\alpha} c^\dagger_{k,\alpha} c_{k,\alpha} + Q \sum_{k,k'} V^\alpha_{k,k'} c^\dagger_{k,\alpha} c_{k',\alpha} \tag{244}$$

with $\alpha = L, R$ and Q the charge on the junction. As usual we study the behavior of the system from its effective action, which is of the type (222) but with a kernel $\alpha(\tau - \tau')$ of the form

$$\alpha(\tau) = \alpha_0 (\frac{\pi K_B T}{sin(\pi k_B T \tau)})^{2-\epsilon} \tag{245}$$

where, as usual, α_0 is given by (215). In the low temperature limit

$$\alpha(\tau) = \alpha_0 \tau^{2-\epsilon} \tag{246}$$

The parameter ϵ characterizes shake-up effects. It can be related to the phase shift δ_L, δ_R in the electronic wavefunction of each electrode produced by the screened Coulomb potential by [47]

$$\epsilon = 2(\frac{\delta_R + \delta_L}{\pi}) - (\frac{\delta_R}{\pi})^2 - (\frac{\delta_L}{\pi})^2 \tag{247}$$

For small positive δ_α, there is a competition between excitonic effects associated with $2(\delta_R + \delta_L)/\pi$ and orthogonality effects associated with $-(\delta_R/\pi)^2 - (\delta_L/\pi)^2$. Notice that δ_R will be positive if the perturbation tends to keep the tunneled electron in the electrode near the tunneling site, as a result of the attraction to the positive electrode. Similarly δ_L will be positive if the hole is attracted to the negatively charged electrode.

The system can again be mapped onto a long range XY model, but now the interaction decays as $\sim \tau^{2-\epsilon}$. Thus its critical behavior can be studied within the framework of renormalization group [37] . The scaling equation for $\alpha \gg 1$ and small ϵ

$$\frac{d\alpha}{d(ln\omega_c)} = -\frac{2}{\pi^2} + \alpha\epsilon \tag{248}$$

implies the existence of an order-disorder transition along the critical line $\alpha_c = 2/(\pi^2\epsilon)$ for $\epsilon \geq 0$. The model is disordered for $\epsilon < 0$. This corresponds to a metallic -insulator transition from the high α_0 (metallic) phase to the low α_0 (insulating) one.

REFERENCES

1. *Single Charge Tunneling, NATO ASI Series, Vol. B*, 294, eds. Grabert H. and Devoret M.H., New York, Plenum Press 1992.
2. Averin D.V. and Likharev K.K. in *Mesoscopic Phenomena in Solids*, edited by Altshuler B.L., Lee P.A. and Webb R.A. Elsevier, Amsterdam 1991.
3. Beenakker C.W.J., *Phys. Rev. B*, **44**, 1646 (1991).
4. Beenakker C.W.J., van Houlen H. and Staring A.A.M. in *Single Charge Tunneling* in ref. [1].
5. Kouwenhoven L.P., Markus C.M., McEuen P.L., Tarucha S., Westervelt R.M. and Wingreen N.S. in *Mesoscopic Electron Transport* , edited by Sohn L.L., Kouwenhoven L.P. and Schön G., Nato ASI Series E: Applied Sciences- Vol-345.
6. Zeller H.R. and Graver I., *Phys. Rev.*, **181**, 789 (1965).
7. Kulik I.O. and Shekhler R.I., *Zh. Eksp. Teor. Fiz., (Sos. Phys. JEPT)*, **68**, 623 (1975).
8. Ingold and Nazarov in *Single Charge Tunneling* in ref. [1].
9. Mesoscopic Superconductivity, Proceedings of the NATO ARW, edited by Mekking F.W., Schön G. and Averin D.V. *Physica B*, 203 (1994).
10. Fazio R. and Schön G. in *Mesoscopic Electron Transport* in ref. [5].
11. Averin D.V. and Likharev K.K., *J. Low Temp. Phys.* , **62** (1986).
12. Schön G. and Zaikin A.D., *Phys. Rep.*, **198**, 237 (1990).
13. Ben-Jacob E. and Gefen Y., *Phys. Lett.* **108 A**, 289 (1985).
14. Grabert H., *Phys. Rev. B*, **50**, 17364 (1994).
15. Garcia N. and Guinea F., *Phys. Rev. B*, **46**, 571 (1992);
16. Garcia N. and Guinea F., *Phys. Rev. B*, **57**, 1398 (1998).
17. Ben-Jacob E., Mottola E. and Schön G., *Phys. Rev. Lett.*, **51**, 2064 (1983).
18. Averin D.V. and Nazarov in *Single Charge Tunneling* in ref. [1].
19. König J., Schoeller H. and Schön G., *Phys. Rev. Lett.*, **78**, 4482 (1997).
20. Pothier H. et al., *Physica B*, **169**, 573 (1991); *Europhys. Lett.*, **17**, 249 (1992).
21. Kouwenhoven L.P., Schön G. and Sohn L.L. in *Mesoscopic Electron Transport* p. 1 and references therein. Ref. [5].
22. Kouwenhoven L.P., Johnson A.T., van der Vaart N.C., Harmans C.J.P.M. and Foxon C.T., *Phys. Rev. Lett.*, **67**, 1626 (1991).
23. Goldhaber-Gordon D., Shtrikman H., Mahaln D., Abush-Magder D., Meirav U. and Kastner M.A., *Nature*, **391**, 156 (1998).
24. Estève D., Pothier H., Guéron S., Birge N.O. and Devoret M.H. in *Mesoscopic Electron Transport* ref. [5].
25. Scott-Thomas J.H.F., Field S.B., Kastner M.A., Smith H.I. and Antoniadis D.A., *Phys. Rev. Lett.*, **62**, 583 (1989).
26. Field S.B., Kastner M.A., Meirav U., Scott-Thomas J.H.F., Antoniadis D.A., Smith H.I. and Wind S.J., *Phys. Rev. B*, **42**, 3523 (1990).
27. Meirav U., Kastner M.A., Heiblum H. and Wind S.J., *Phys. Rev. B*, **40**, 5871 (1989).
28. Meirav U., Kastner M.A. and Wind S.J., *Phys. Rev. Lett.*, **65**, 771 (1990).
29. Kastner M.A., *Rev. of Mod. Phys.*, **64**, 849 (1992).
30. Widom A., Megaloudis G., Clark T.D., Prance H. and Prance R.J., *J. Phys. A*, **15**,

3877 (1982).
31. Likharev K.K. and Zorin A.B., *J. Low Temp. Phys.*, **59**, 347 (1985).
32. Guinea F. and Schön G., *Europhys. Lett.*, **1**, 585-593 (1986); *J. Low Temp. Phys.*, **69**, 219 (1987).
33. Schön G. and Zaikin A.D.,*Phys. Rep.*, **198**, 237-412 (1990).
34. Caldeira A.O. and Legget A.J., *Phys. Rev. Lett.*, **46**, 211 (1981); *Annals of Physics*, **149**, 374-456 (1983).
35. Ambegaokar V., Eckern U. and Schön G., *Phys. Rev. Lett.*, **48**, 1745 (1982); Eckern U., Schön G. and Ambegaokar V., *Phys. Rev. Lett.*, **30**, 6419 (1984).
36. Renn S.R., *cond-mat* 9708194. Submitted to PRB.
37. Kosterlitz J.M., *Phys. Rev. Lett.*, **37**, 1577 (1976).
38. Chakravarty S., *Phys. Rev. Lett.*, **49**, 681 (1982).
39. Bray A.J. and Moore M.A., *Phys. Rev. Lett.*, **49**, 1545 (1982).
40. Hakim V., Muramatsu A. and Guinea F., *Phys. Rev. B*, **30**, 464 (1984).
41. Mohanty P., Jariwala E.M.Q. and Webb R.A., *Phys. Rev. Lett.*, **78**, 3366 (1997).
42. Ueda M. and Guinea F., *Z. Phys. B -Condensed Matter*, **85**, 413 (1991).
43. Mahan G.D.,*Many-Particle Physics*, Plenum (New York) 1991.
44. Nozières P. and de Dominicis C.T., *Phys. Rev.*, **178**, 1097 (1969).
45. Anderson P.W.,*Phys. Rev.*,**164**, 352 (1967).
46. T. Strohm and F. Guinea, *Nucl. Phys. B* **487**, 795 (1997).
47. Drewes S., Renn S.R. and Guinea F., *Phys. Rev. Lett.* **80**, 1043 (1998).
48. Ueda M. and Kurihara S. in *Macroscopic Quantum Phenomena*, Clark T.D., Prance H., Prance R.J. and Spiller T.P. (eds), Singapore: World Scientific 1990.